Electronic Supplementary Material (ESI) for Catalysis Science & Technology.

Supplementary Information

Modulating the Water oxidation Catalytic activity of Iridium Complexes by Functionalizing the Cp*-Ancillary Ligand: Hints on the Nature of the Active Species

Giordano Gatto,[a] Alice De Palo,[b] Ana C. Carrasco,[c] Ana M. Pizarro,[c] Stefano Zacchini,[d] Guido Pampaloni,[b] Fabio Marchetti,[b] and Alceo Macchioni*[a]*

[a]Department of Chemistry, Biology and Biotechnology and CIRCC, University of Perugia, Via Elce di Sotto 8, 06123 Perugia, Italy. [b]Dipartimento di Chimica e Chimica Industriale University of Pisa, Via G. Moruzzi 13, 56124 Pisa, Italy. [c]IMDEA Nanociencia, Ciudad Universitaria de Cantoblanco, 28049 Madrid, Spain. [d]Dipartimento di Chimica Industriale "Toso Montanari", Università di Bologna, Viale Risorgimento 4, 40136 Bologna, Italy.

CONTENTS

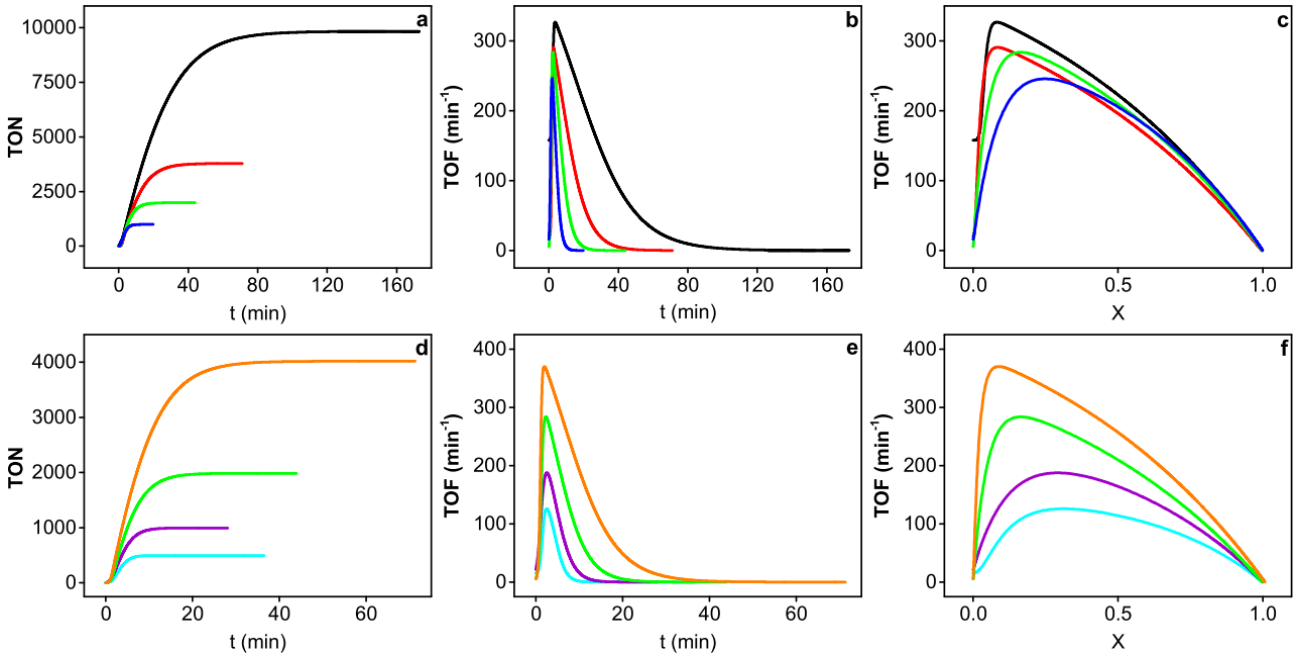

Figure S1: Kinetic trends for catalyst **1** (water solution at pH 7 by phosphate buffer 0.2 M, 25°C) at different iridium (a, b, c: black, 1 μM; red, 2.5 μM; green, 5 μM; blue, 10 μM) and $NaIO_4$ (d, e, f: orange, 40 mM; green, 20 mM; violet, 10 mM; cyan, 5 mM) concentrations.

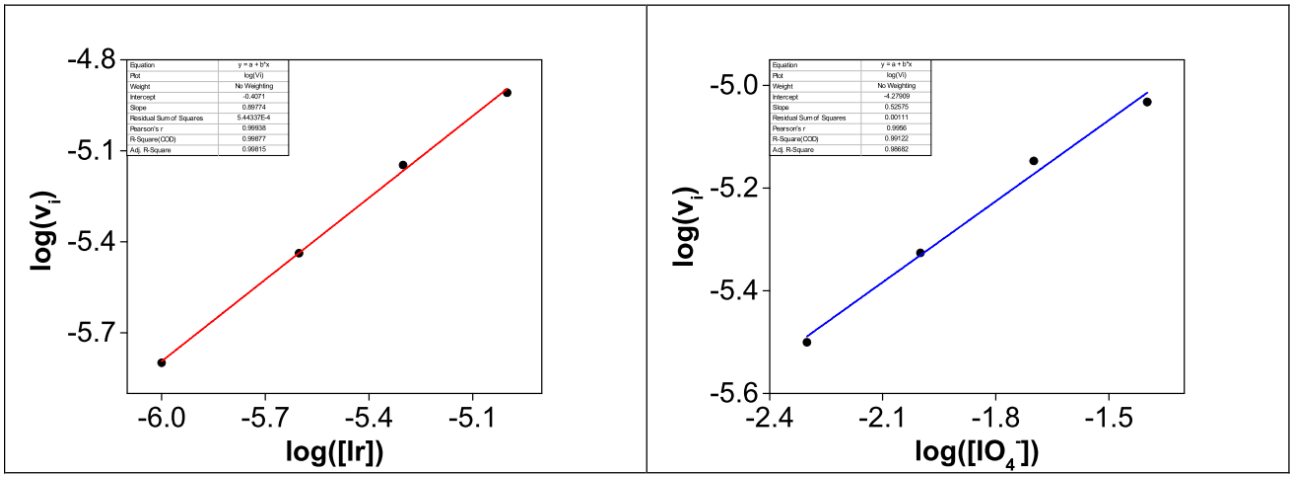

Figure S2: Linear fit of the initial rate method for catalyst **1**. Left: specific order for Ir, right: specific order for $NaIO_4$.

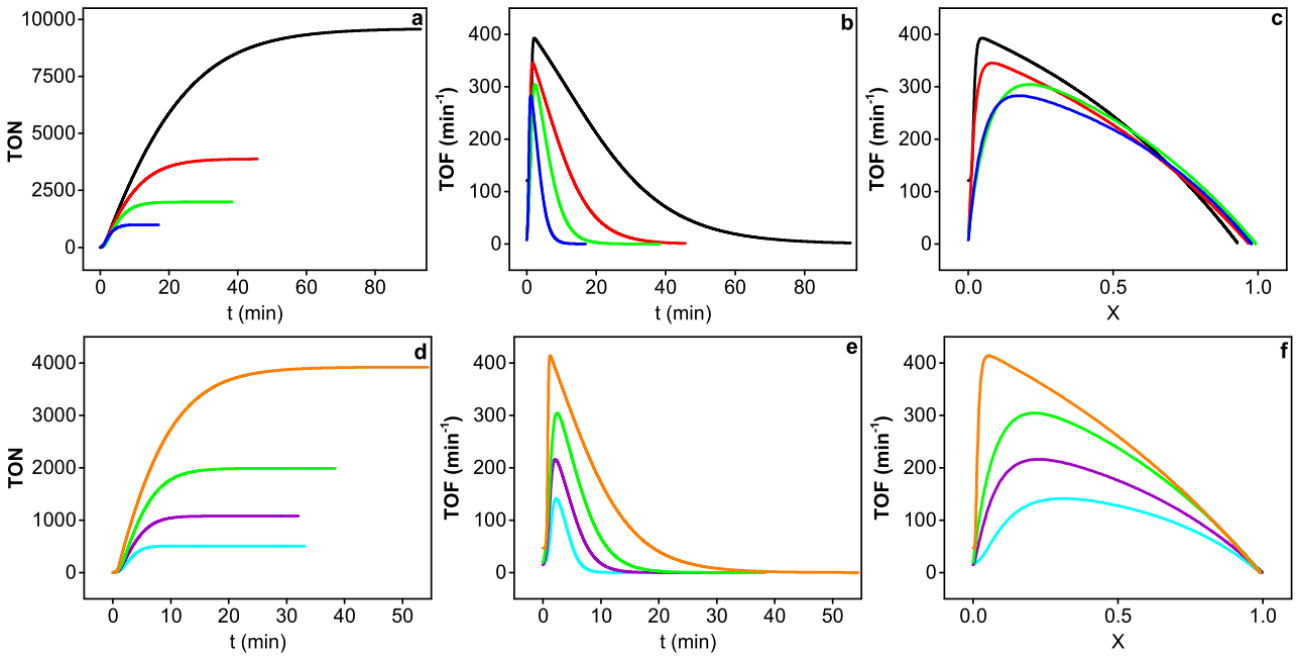

Figure S3: Kinetic trends for catalyst **2** (water solution at pH 7 by phosphate buffer 0.2 M, 25°C) at different iridium (a, b, c: black, 1 μM; red, 2.5 μM; green, 5 μM; blue, 10 μM) and $NaIO_4$ (d, e, f: orange, 40 mM; green, 20 mM; violet, 10 mM; cyan, 5 mM) concentrations.

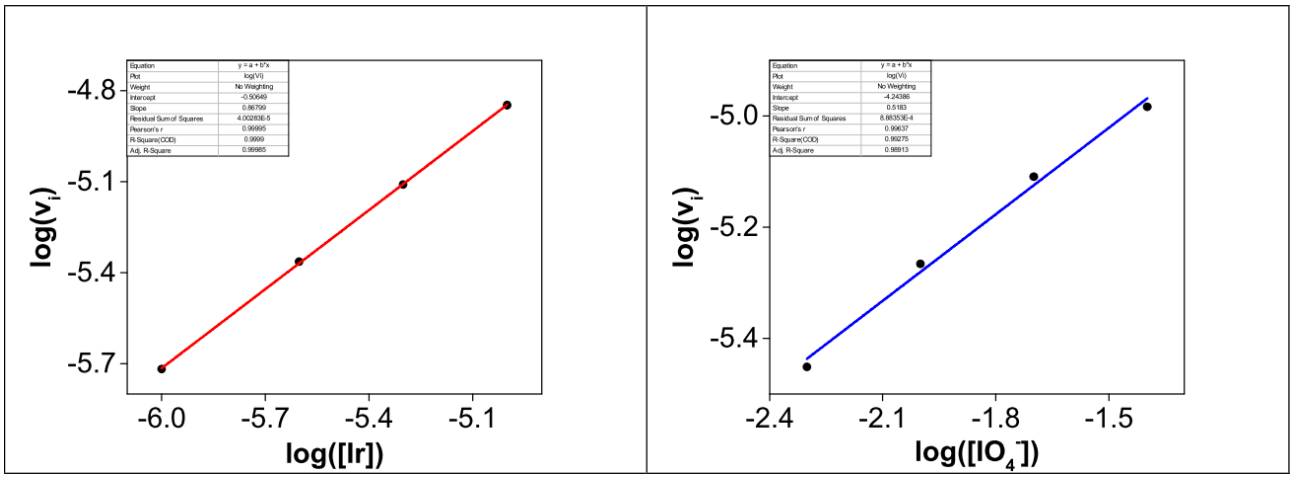

Figure S4: Linear fit of the initial rate method for catalyst **2**. Left: specific order for Ir, right: specific order for $NaIO_4$.

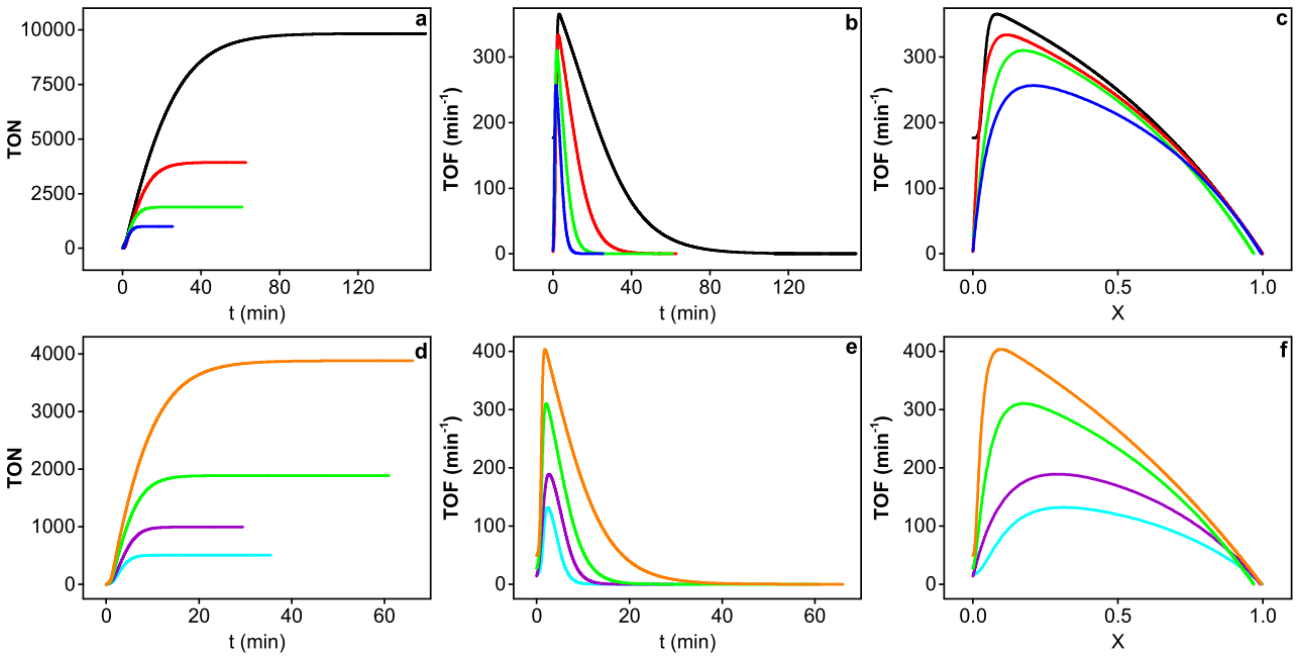

Figure S5: Kinetic trends for catalyst **3** (water solution at pH 7 by phosphate buffer 0.2 M, 25°C) at different iridium (a, b, c: black, 1 μM; red, 2.5 μM; green, 5 μM; blue, 10 μM) and $NaIO_4$ (d, e, f: orange, 40 mM; green, 20 mM; violet, 10 mM; cyan, 5 mM) concentrations.

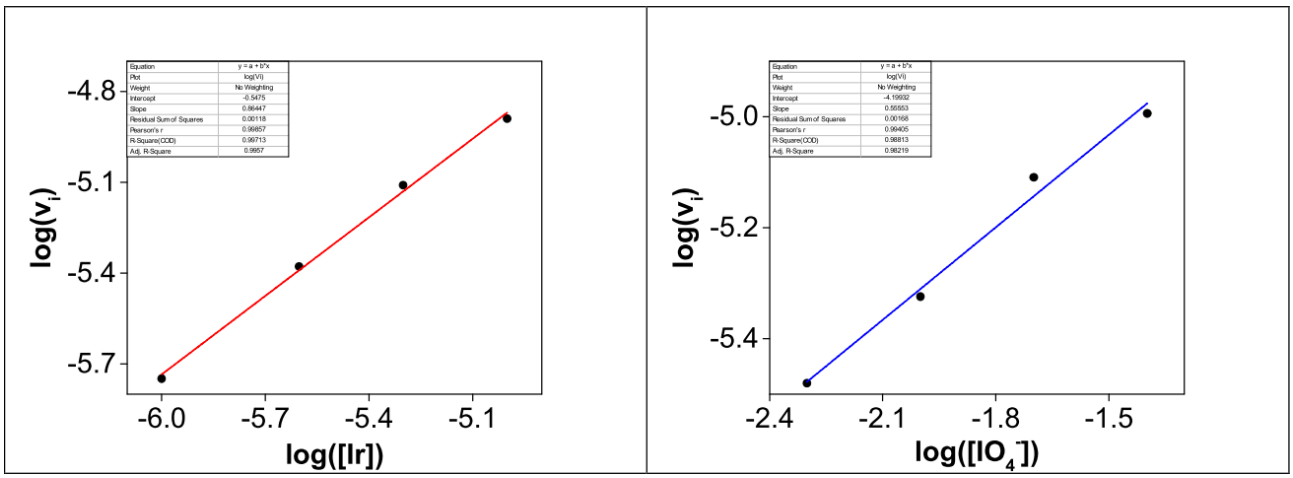

Figure S6: Linear fit of the initial rate method for catalyst **3**. Left: specific order for Ir, right: specific order for $NaIO_4$.

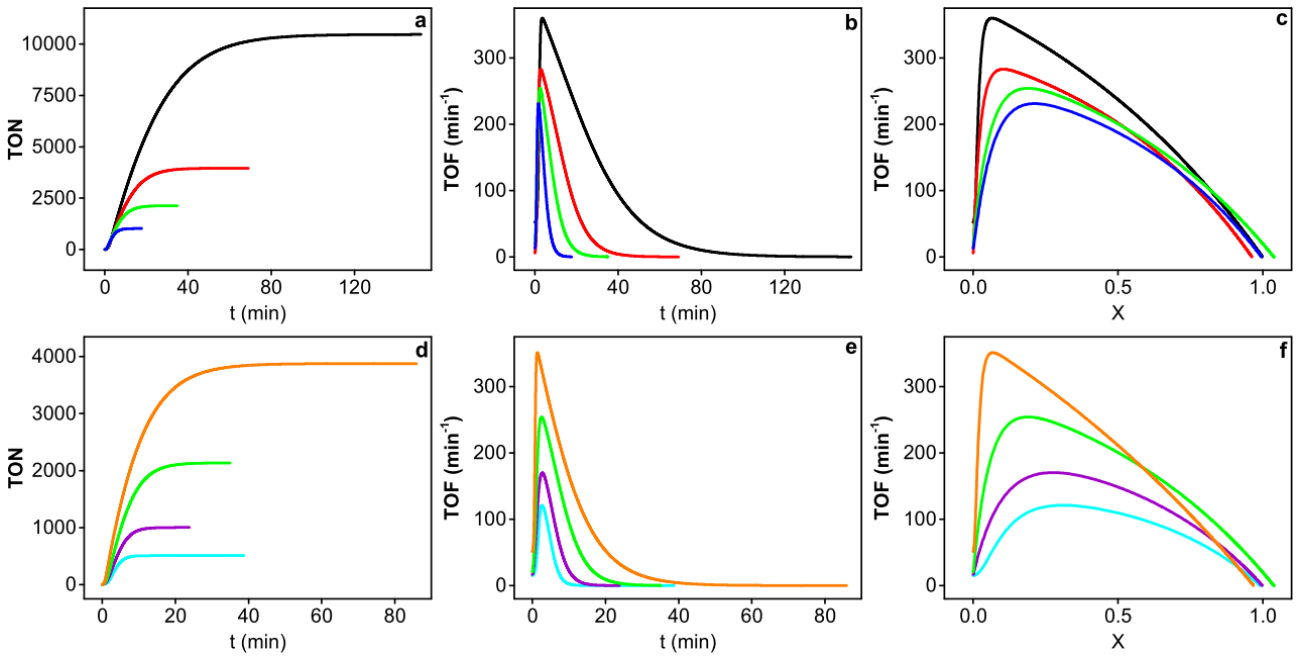

Figure S7: Kinetic trends for catalyst **4** (water solution at pH 7 by phosphate buffer 0.2 M, 25°C) at different iridium (a, b, c: black, 1 μM; red, 2.5 μM; green, 5 μM; blue, 10 μM) and $NaIO_4$ (d, e, f: orange, 40 mM; green, 20 mM; violet, 10 mM; cyan, 5 mM) concentrations.

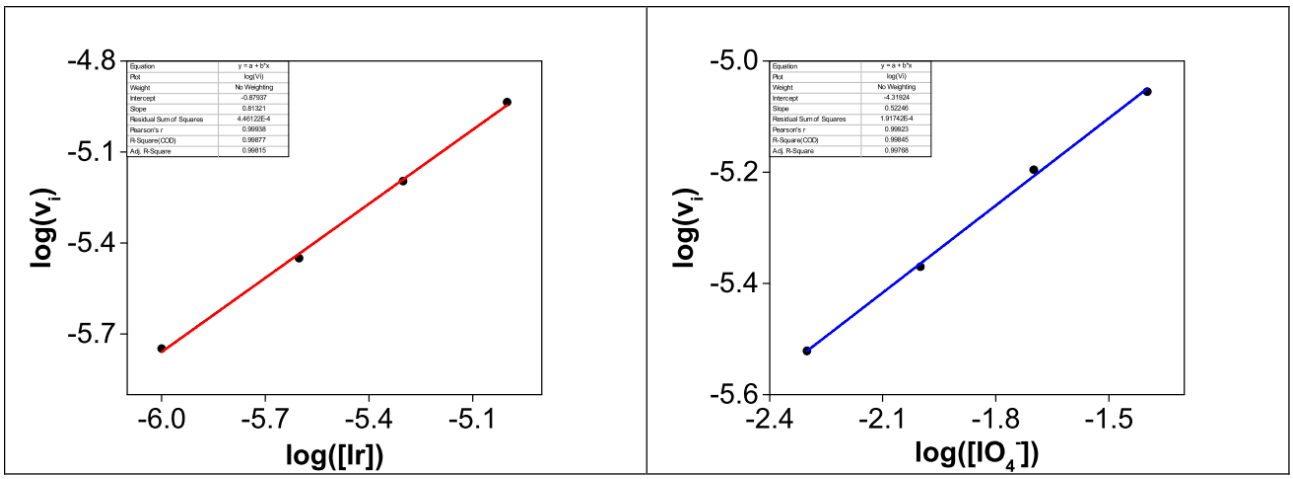

Figure S8: Linear fit of the initial rate method for catalyst **4**. Left: specific order for Ir, right: specific order for $NaIO_4$.

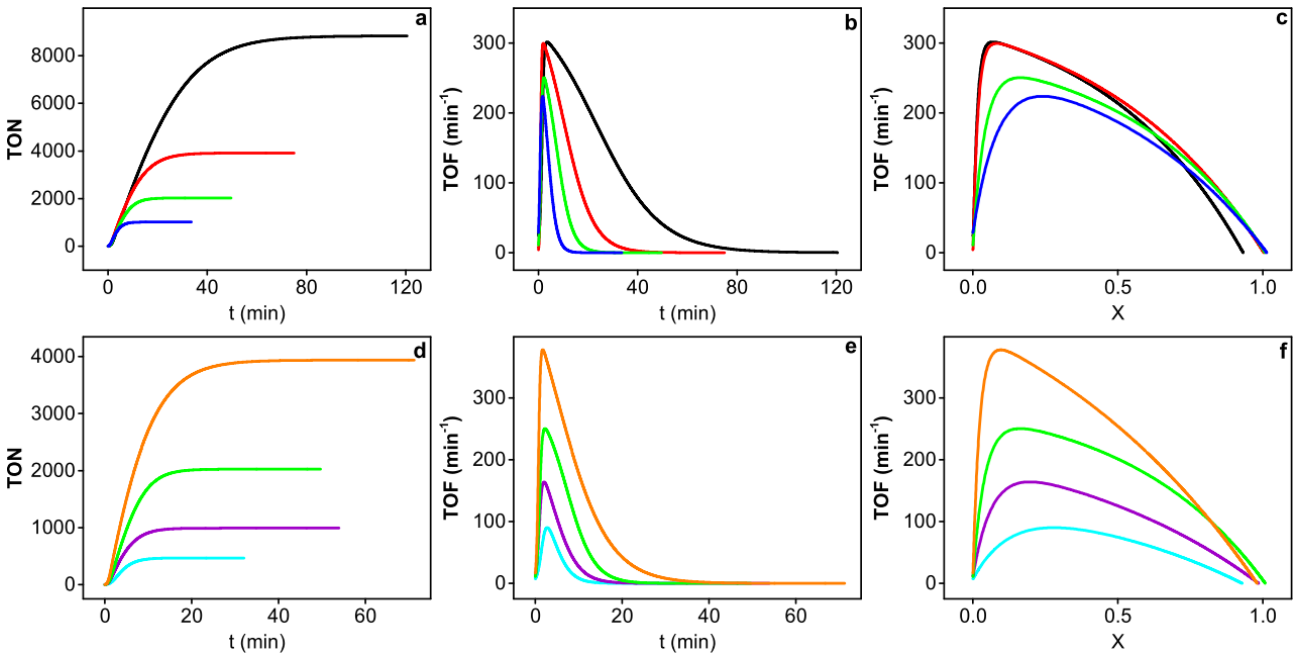

Figure S9: Kinetic trends for catalyst **5** (water solution at pH 7 by phosphate buffer 0.2 M, 25°C) at different iridium (a, b, c: black, 1 μM; red, 2.5 μM; green, 5 μM; blue, 10 μM) and $NaIO_4$ (d, e, f: orange, 40 mM; green, 20 mM; violet, 10 mM; cyan, 5 mM) concentrations.

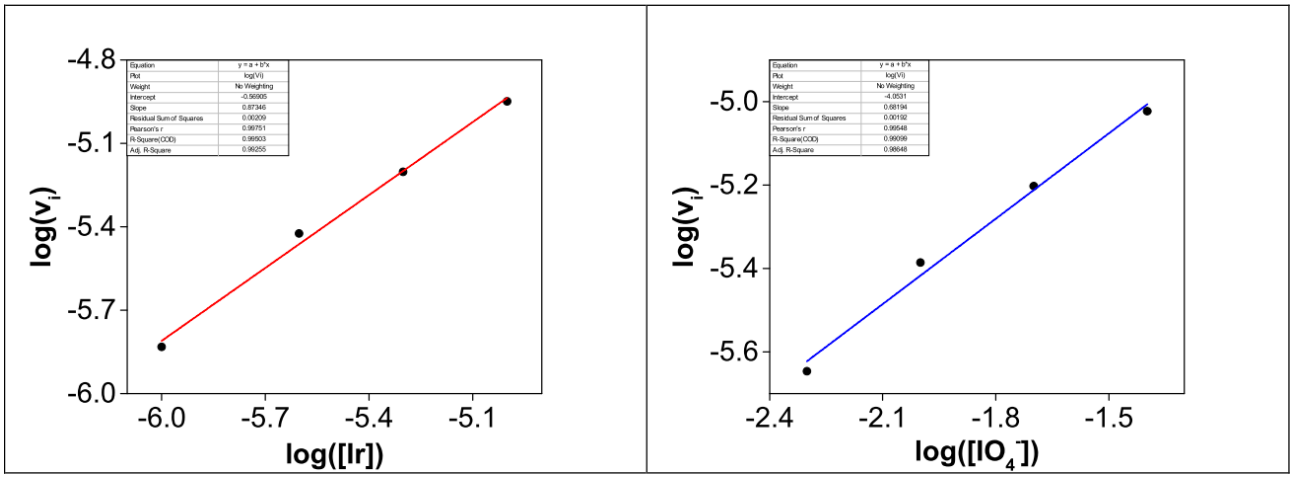

Figure S10: Linear fit of the initial rate method for catalyst **5**. Left: specific order for Ir, right: specific order for $NaIO_4$.

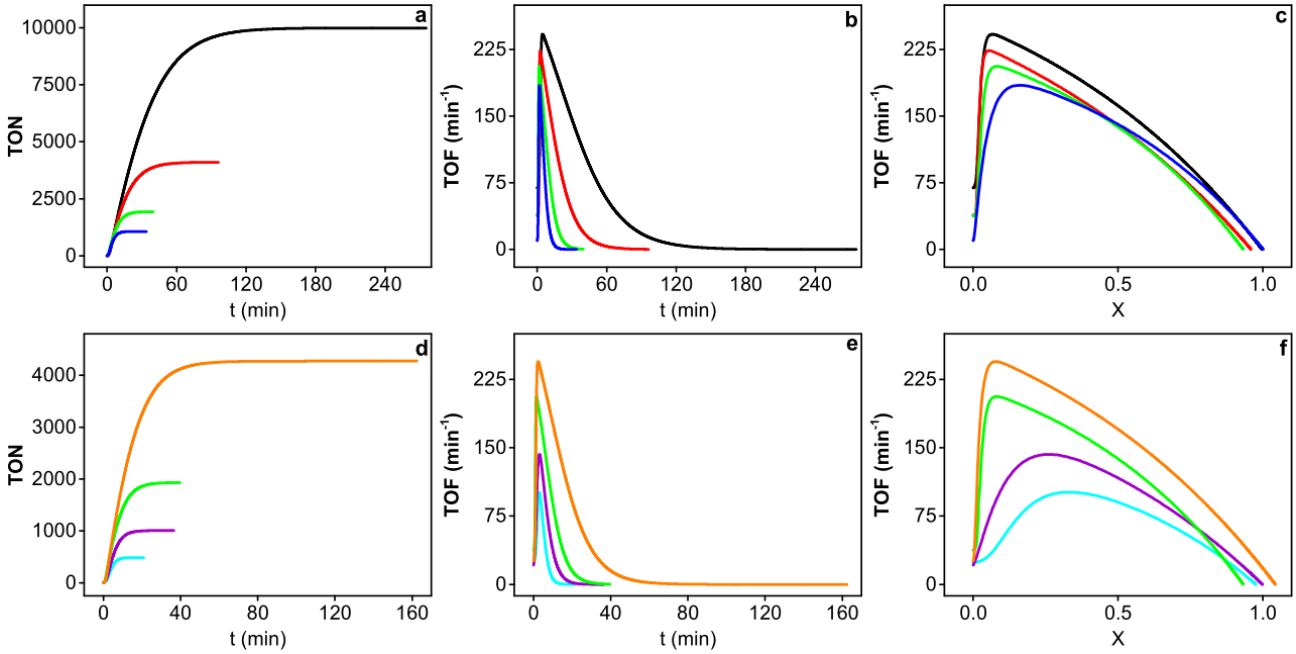

Figure S11: Kinetic trends for catalyst **6** (water solution at pH 7 by phosphate buffer 0.2 M, 25°C) at different iridium (a, b, c: black, 1 µM; red, 2.5 µM; green, 5 µM; blue, 10 µM) and $NaIO_4$ (d, e, f: orange, 40 mM; green, 20 mM; violet, 10 mM; cyan, 5 mM) concentrations.

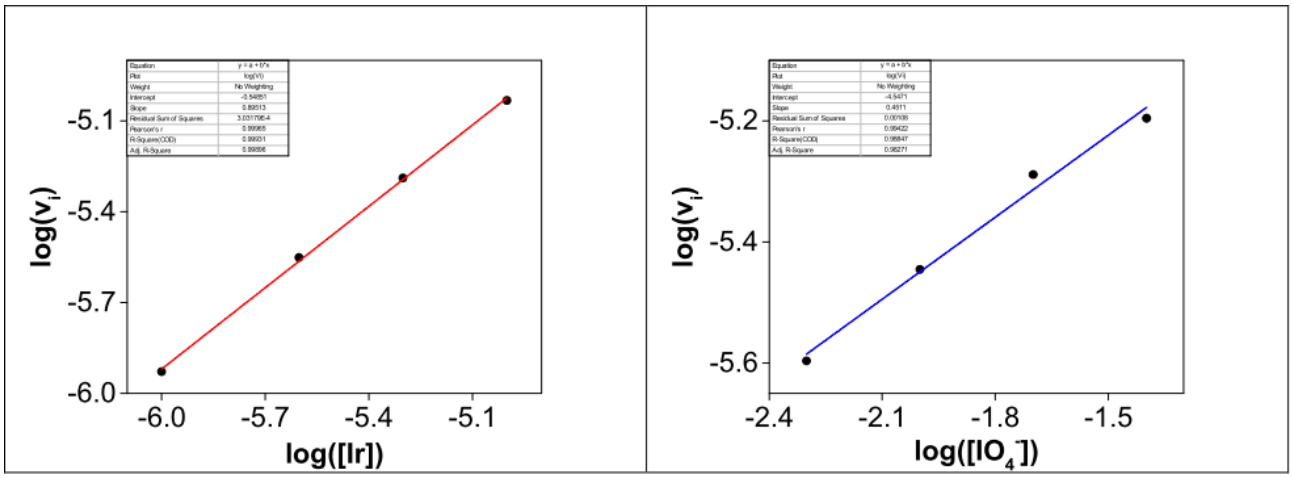

Figure S12: Linear fit of the initial rate method for catalyst **6**. Left: specific order for Ir, right: specific order for $NaIO_4$.

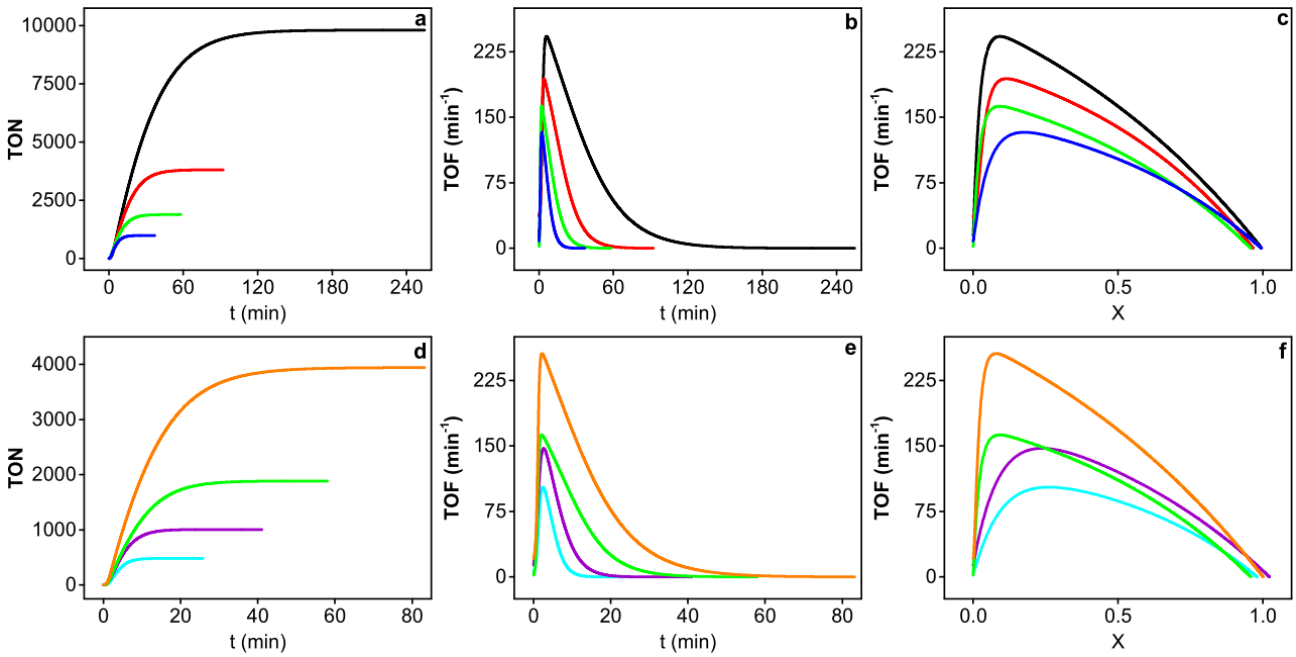

Figure S13: Kinetic trends for catalyst **7** (water solution at pH 7 by phosphate buffer 0.2 M, 25°C) at different iridium (a, b, c: black, 1 µM; red, 2.5 µM; green, 5 µM; blue, 10 µM) and $NaIO_4$ (d, e, f: orange, 40 mM; green, 20 mM; violet, 10 mM; cyan, 5 mM) concentrations.

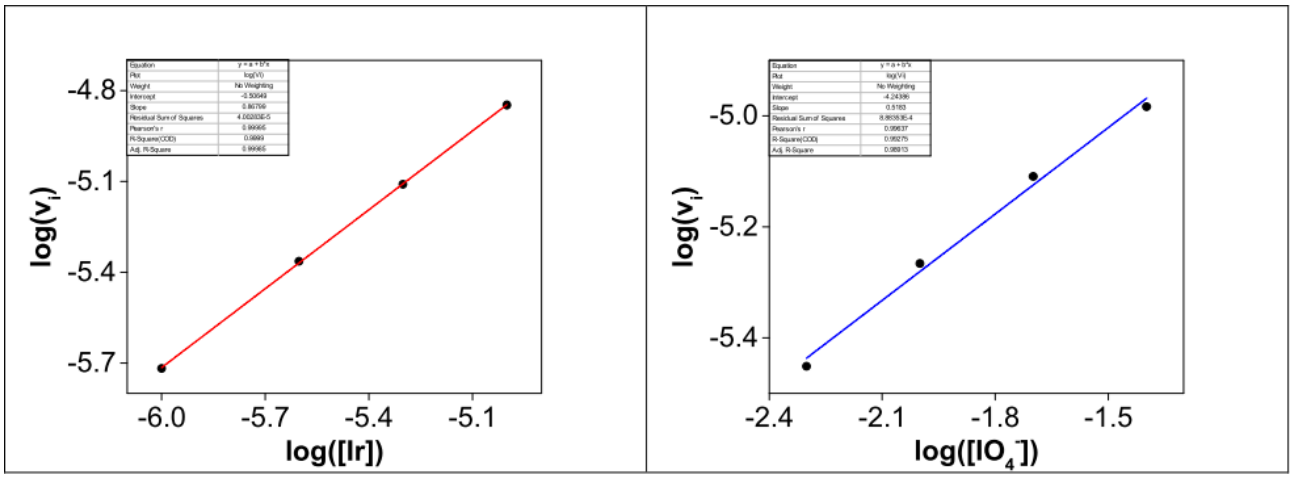

Figure S14: Linear fit of the initial rate method for catalyst **7**. Left: specific order for Ir, right: specific order for $NaIO_4$.

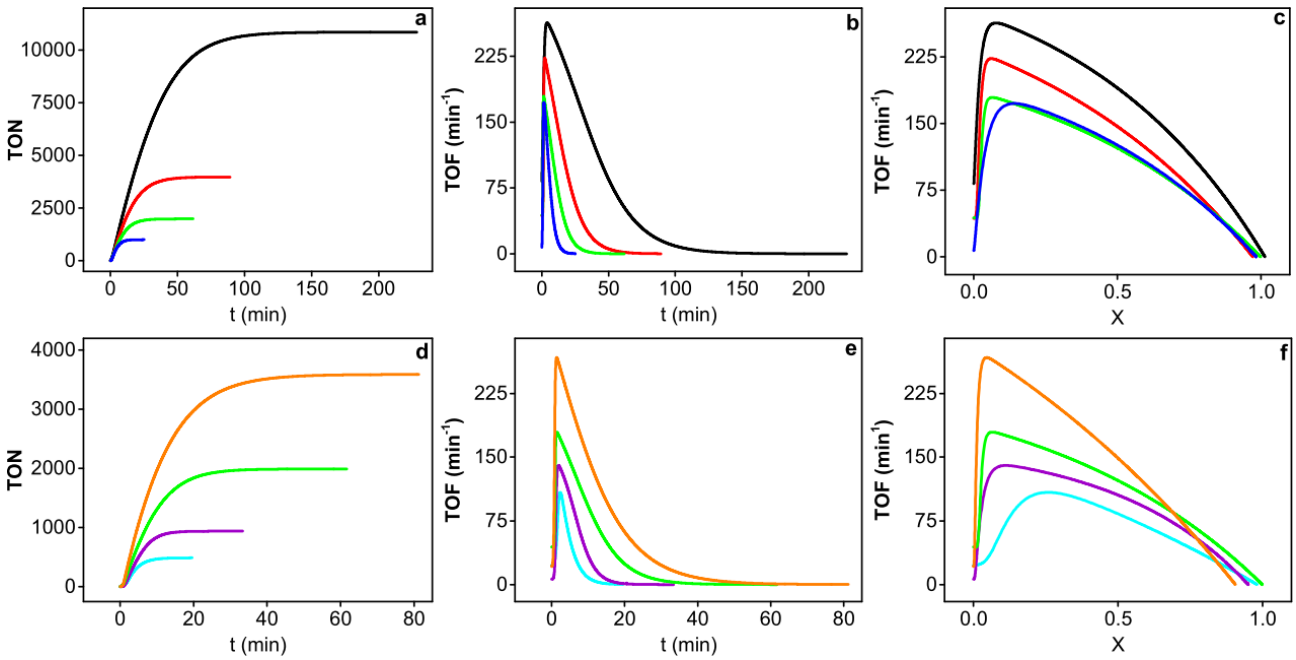

Figure S15: Kinetic trends for catalyst **8** (water solution at pH 7 by phosphate buffer 0.2 M, 25°C) at different iridium (a, b, c: black, 1 µM; red, 2.5 µM; green, 5 µM; blue, 10 µM) and $NaIO_4$ (d, e, f: orange, 40 mM; green, 20 mM; violet, 10 mM; cyan, 5 mM) concentrations.

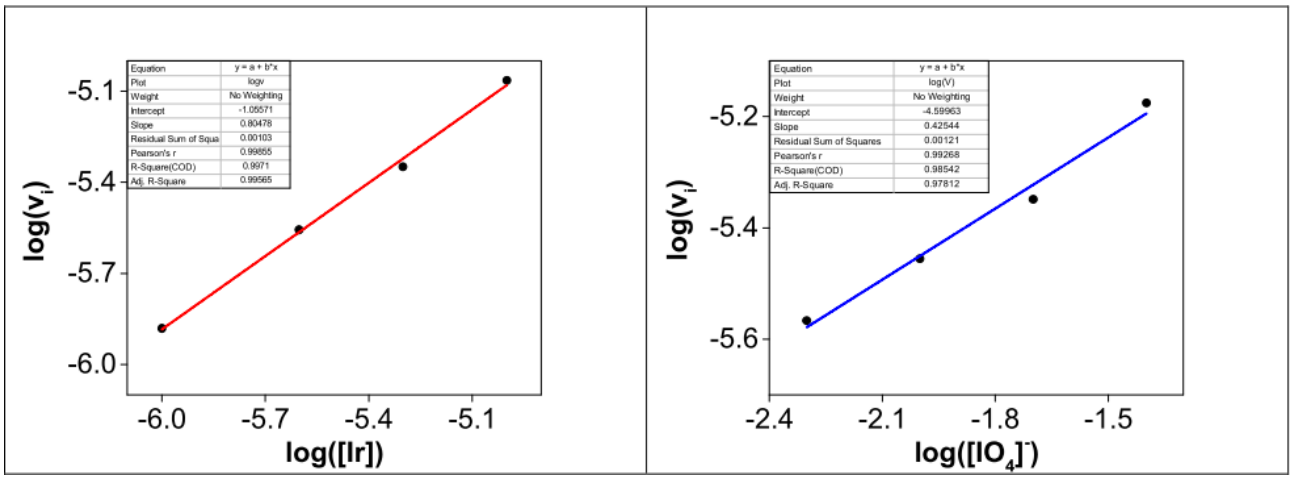

Figure S16: Linear fit of the initial rate method for catalyst **8**. Left: specific order for Ir, right: specific order for $NaIO_4$.

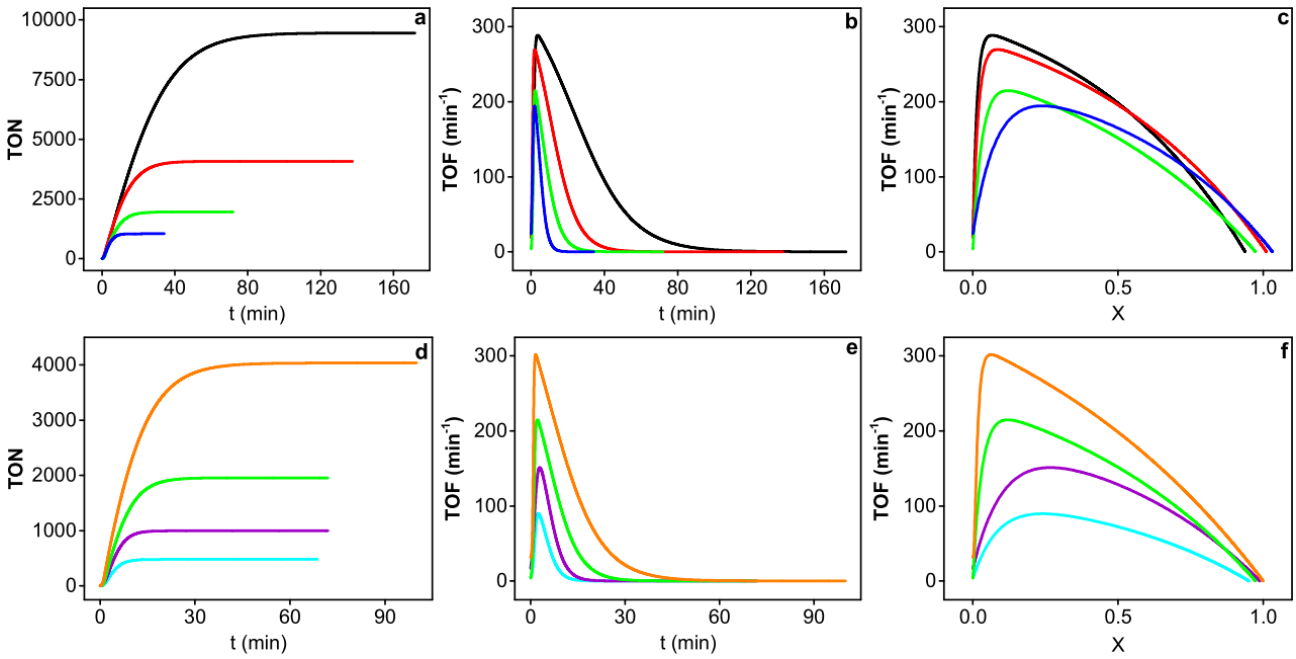

Figure S17: Kinetic trends for catalyst **9** (water solution at pH 7 by phosphate buffer 0.2 M, 25°C) at different iridium (a, b, c: black, 1 µM; red, 2.5 µM; green, 5 µM; blue, 10 µM) and $NaIO_4$ (d, e, f: orange, 40 mM; green, 20 mM; violet, 10 mM; cyan, 5 mM) concentrations.

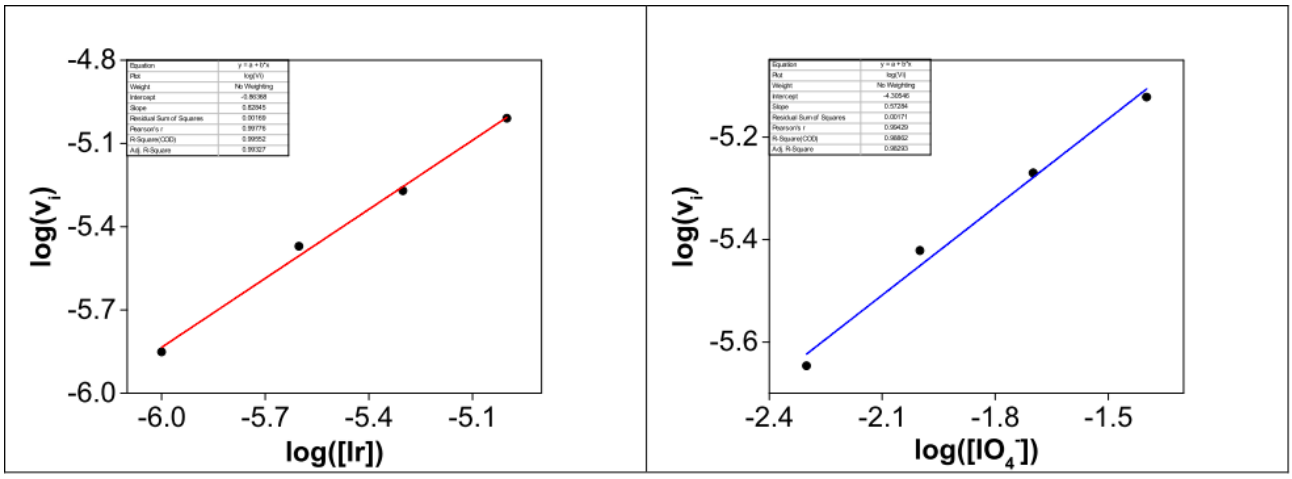

Figure S18: Linear fit of the initial rate method for catalyst **9**. Left: specific order for Ir, right: specific order for $NaIO_4$.

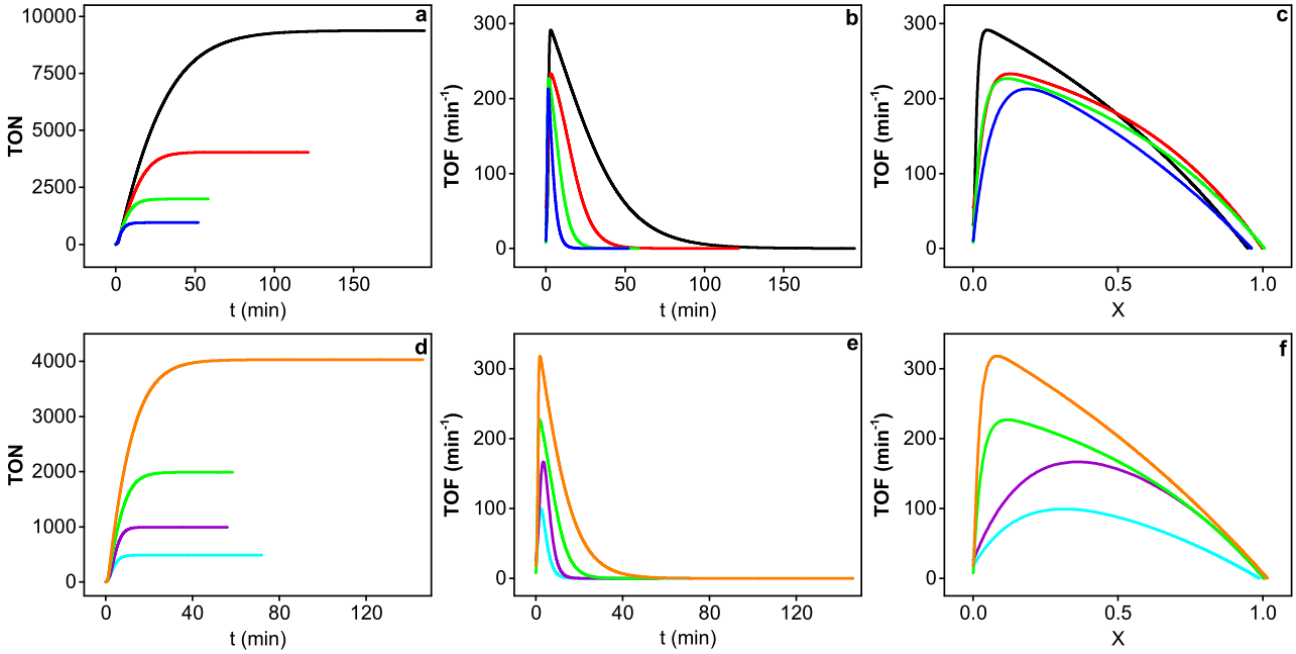

Figure S19: Kinetic trends for catalyst **10** (water solution at pH 7 by phosphate buffer 0.2 M, 25°C) at different iridium (a, b, c: black, 1 µM; red, 2.5 µM; green, 5 µM; blue, 10 µM) and $NaIO_4$ (d, e, f: orange, 40 mM; green, 20 mM; violet, 10 mM; cyan, 5 mM) concentrations.

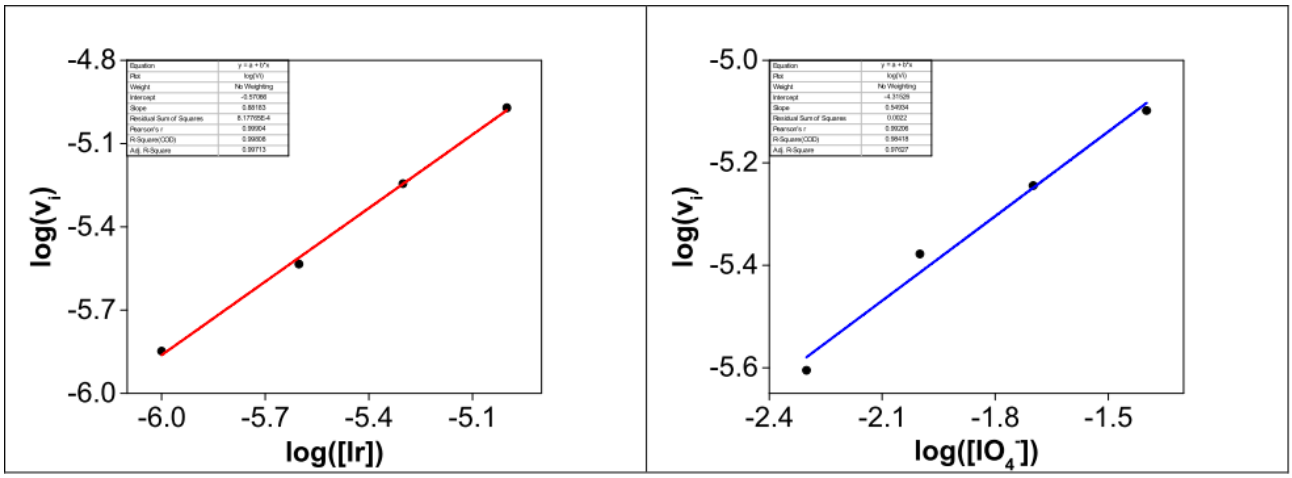

Figure S20: Linear fit of the initial rate method for catalyst **10**. Left: specific order for Ir, right: specific order for $NaIO_4$.

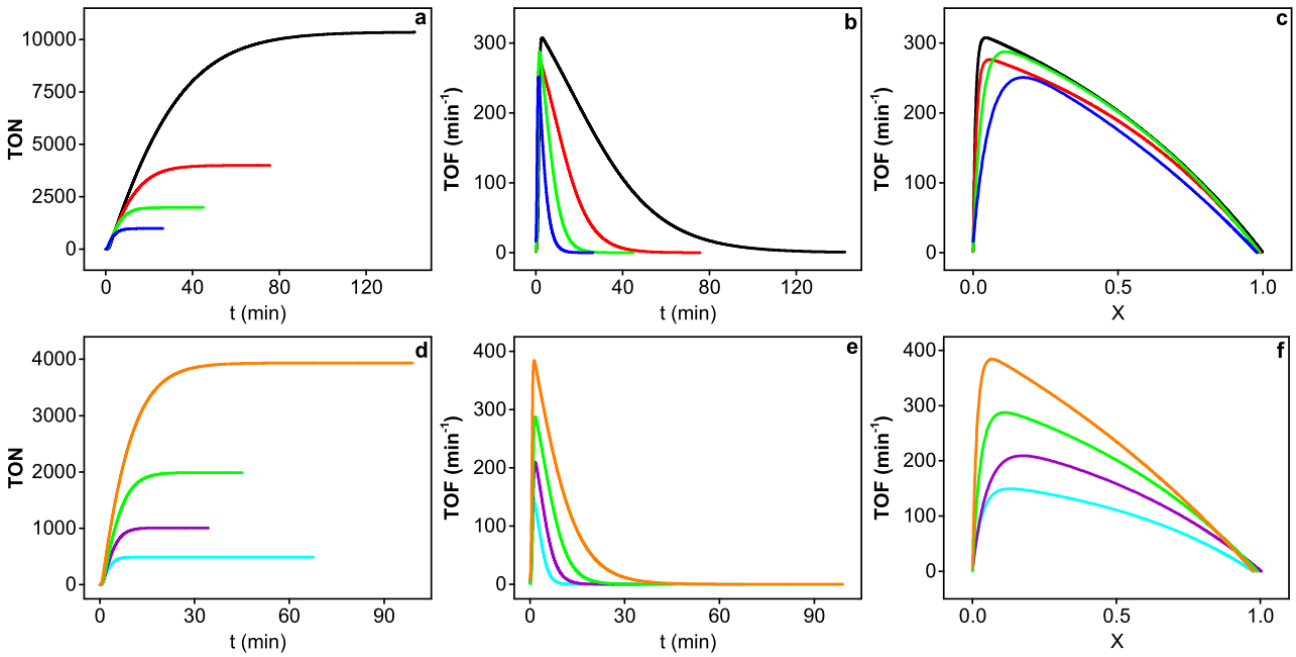

Figure S21: Kinetic trends for catalyst **12** (water solution at pH 7 by phosphate buffer 0.2 M, 25°C) at different iridium (a, b, c: black, 1 µM; red, 2.5 µM; green, 5 µM; blue, 10 µM) and $NaIO_4$ (d, e, f: orange, 40 mM; green, 20 mM; violet, 10 mM; cyan, 5 mM) concentrations.

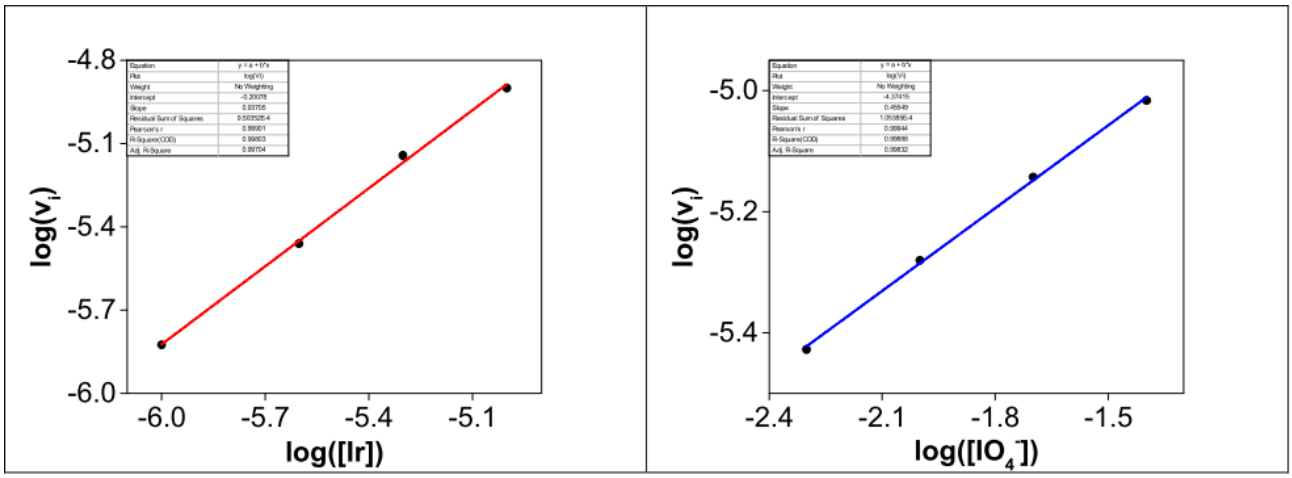

Figure S22: Linear fit of the initial rate method for catalyst **12**. Left: specific order for Ir, right: specific order for $NaIO_4$.

Table S1. Summary of kinetic and catalytic performances of catalysts **1**–**3** (water solution at pH 7 by phosphate buffer, 25°C).

Experiment	[Cat] (μM)	[$NaIO_4$] (mM)	$TOF_{max}(X)$ (min^{-1})	TON	Yield (%)
			$[(\eta^5\text{-}C_5Me_4H)IrCl_2]_2$ (**1**)		
1	1.0	20.0	327 ± 33 (0.08)	9829 ± 492	100
2	2.5	20.0	291 ± 29 (0.09)	3783 ± 189	98
3	5.0	20.0	284 ± 28 (0.16)	1985 ± 99	100
4	10.0	20.0	245 ± 25 (0.25)	994 ± 50	100
5	5.0	5.0	126 ± 13 (0.24)	497 ± 25	100
6	5.0	10.0	188 ± 19 (0.29)	994 ± 50	100
7	5.0	40.0	360 ± 36 (0.09)	4017 ± 201	101*
			$[Cp^*IrCl_2]_2$ (**2**)		
1	1.0	20.0	393 ± 39 (0.05)	9575 ± 479	93
2	2.5	20.0	345 ± 35 (0.08)	3878 ± 194	97
3	5.0	20.0	304 ± 30 (0.21)	2000 ± 100	98
4	10.0	20.0	283 ± 28 (0.18)	993 ± 50	99
5	5.0	5.0	141 ± 14 (0.31)	507 ± 25	99
6	5.0	10.0	216 ± 22 (0.23)	1079 ± 54	99
7	5.0	40.0	414 ± 41 (0.06)	3920 ± 196	99
			$[(\eta^5\text{-}C_5Me_4Et)IrCl_2]_2$ (**3**)		
1	1.0	20.0	360 ± 36 (0.08)	9829 ± 492	99
2	2.5	20.0	334 ± 33 (0.12)	3935 ± 197	100
3	5.0	20.0	310 ± 31 (0.18)	1889 ± 95	97
4	10.0	20.0	257 ± 26 (0.21)	1001 ± 50	100
5	5.0	5.0	132 ± 13 (0.31)	507 ± 25	100
6	5.0	10.0	189 ± 19 (0.29)	996 ± 50	100
7	5.0	40.0	404 ± 40 (0.10)	3883 ± 194	99
8	5.0	20.0	302 ± 30 (0.12)	1944 ± 97	100
8’	5.0	20.0	120 ± 12 (0.15)	1955 ± 98	100

Table S2. Summary of kinetic and catalytic performances of catalysts **4**–**6** (water solution at pH 7 by phosphate buffer, 25°C).

Experiment	[Cat] (μM)	[$NaIO_4$] (mM)	TOF_{max}(X) (min^{-1})	TON	Yield (%)
			$[(\eta^5\text{-}C_5Me_4{}^nPr)IrCl_2]_2$ (**4**)		
1	1.0	20.0	366 ± 37 (0.07)	10463 ± 523	100
2	2.5	20.0	283 ± 28 (0.11)	3960 ± 198	96
3	5.0	20.0	254 ± 25 (0.19)	2135 ± 107	104*
4	10.0	20.0	231 ± 23 (0.21)	1024 ± 51	100
5	5.0	5.0	121 ± 12 (0.31)	507 ± 25	100
6	5.0	10.0	170 ± 17 (0.27)	1002 ± 50	99
7	5.0	40.0	251 ± 25 (0.07)	3878 ± 194	97
			$[(\eta^5\text{-}C_5Me_4CH_2CH_2NH_2{\cdot}HCl)IrCl_2]_2$ (**5**)		
1	1.0	20.0	302 ± 30 (0.07)	8826 ± 441	93
2	2.5	20.0	300 ± 30 (0.08)	3915 ± 196	100
3	5.0	20.0	250 ± 25 (0.16)	2026 ± 101	101*
4	10.0	20.0	224 ± 22 (0.24)	1018 ± 51	101*
5	5.0	5.0	90 ± 9 (0.24)	465 ± 23	93
6	5.0	10.0	164 ± 16 (0.20)	990 ± 50	99
7	5.0	40.0	378 ± 38 (0.10)	3938 ± 197	98
			$[(\eta^5\text{-}C_5Me_4Ph)IrCl_2]_2$ (**6**)		
1	1.0	20.0	263 ± 26 (0.07)	9994 ±	100
2	2.5	20.0	222 ± 22 (0.05)	4100 ±	99
3	5.0	20.0	180 ± 18 (0.08)	1932 ±	93
4	10.0	20.0	173 ± 17 (0.16)	1064 ±	100
5	5.0	5.0	109 ± 11 (0.33)	487 ±	99
6	5.0	10.0	140 ± 14 (0.26)	1007 ±	100
7	5.0	40.0	267 ± 27 (0.08)	4271 ±	104*

Table S3. Summary of kinetic and catalytic performances of catalysts **7**–**9** (water solution at pH 7 by phosphate buffer, 25°C).

Experiment	[Cat] (μM)	[$NaIO_4$] (mM)	TOF_{max}(X) (min^{-1})	TON	Yield (%)
			[{η^5-C_5Me_4(4-C_6H_4F}$IrCl_2$]$_2$ (**7**)		
1	1.0	20.0	242 ± 24 (0.09)	9802 ± 490	99
2	2.5	20.0	194 ± 19 (0.12)	3805 ± 195	97
3	5.0	20.0	163 ± 16 (0.09)	1887 ± 94	96
4	10.0	20.0	133 ± 13 (0.18)	989 ± 50	99
5	5.0	5.0	103 ± 10 (0.26)	482 ± 24	98
6	5.0	10.0	147 ± 15 (0.24)	1007 ± 50	102*
7	5.0	40.0	256 ± 26 (0.08)	3941 ± 197	100
			[{η^5-C_5Me_4(4-C_6H_4OH}$IrCl_2$]$_2$ (**8**)		
1	1.0	20.0	263 ± 26 (0.08)	10857 ± 543	101*
2	2.5	20.0	223 ± 22 (0.06)	3968 ± 198	97
3	5.0	20.0	179 ± 18 (0.07)	1991 ± 100	99
4	10.0	20.0	173 ± 17 (0.14)	1003 ± 50	98
5	5.0	5.0	109 ± 11 (0.26)	489 ± 25	98
6	5.0	10.0	140 ± 14 (0.11)	939 ± 47	95
7	5.0	40.0	267 ± 27 (0.05)	3588 ± 179	91
			[(η^5-C_5Me_4Bn)$IrCl_2$]$_2$ (**9**)		
1	1.0	20.0	289 ± 29 (0.07)	9456 ± 473	94
2	2.5	20.0	270 ± 27 (0.09)	4078 ± 204	97
3	5.0	20.0	214 ± 21 (0.12)	1956 ± 98	101*
4	10.0	20.0	194 ± 19 (0.24)	1040 ± 52	103*
5	5.0	5.0	90 ± 9 (0.24)	480 ± 24	95
6	5.0	10.0	151 ± 15 (0.27)	997 ± 50	99
7	5.0	40.0	302 ± 30 (0.06)	4033 ± 202	100
8	5.0	20.0	217 ± 22 (0.14)	2023 ± 101	100
8’	5.0	20.0	99 ± 10 (0.12)	1901 ± 95	94

Table S4. Summary of kinetic and catalytic performances of catalysts **10–12** (water solution at pH 7 by phosphate buffer, 25°C).

Experiment	[Cat] (μM)	[$NaIO_4$] (mM)	$TOF_{max}(X)$ (min^{-1})	TON	Yield (%)
			[(η^5-C_5Me_4H)Ir(pic)Cl] (**10**)		
1	1.0	20.0	292 ± (0.05)	9397 ± 480	95
2	2.5	20.0	233 ± (0.13)	4044 ± 202	100
3	5.0	20.0	227 ± (0.12)	1988 ± 99	100
4	10.0	20.0	213 ± (0.19)	951 ± 48	96
5	5.0	5.0	99 ± (0.31)	489 ± 25	99
6	5.0	10.0	167 ± (0.36)	993 ± 50	100
7	5.0	40.0	318 ± (0.08)	4028 ± 201	102*
			[Cp*Ir(pic)NO_3]		
1	1.0	20.0	300 ± 26 (0.11)	9244 ± 472	92
2	2.5	20.0	275 ± 24 (0.16)	4054 ± 207	100
3	5.0	20.0	288 ± 25 (0.11)	1949 ± 99	98
4	10.0	20.0	283 ± 25 (0.11)	944 ± 48	95
5	5.0	5.0	165 ± 15 (0.08)	466 ± 24	94
6	5.0	10.0	230 ± 20 (0.15)	957 ± 49	96
7	5.0	40.0	465 ± 41 (0.06)	3711 ± 189	94
			[(η^5-$C_5Me_4{}^nPr$)Ir(pic)Cl] (**11**)		
1	1.0	20.0	307 ± 31 (0.04)	10346 ± 517	100
2	2.5	20.0	276 ± 28 (0.06)	3996 ± 199	99
3	5.0	20.0	287 ± 29 (0.11)	1991 ± 100	99
4	10.0	20.0	250 ± 25 (0.17)	987 ± 49	98
5	5.0	5.0	150 ± 15 (0.13)	491 ± 25	98
6	5.0	10.0	209 ± 21 (0.18)	1009 ± 50	100
7	5.0	40.0	384 ± 38 (0.07)	3934 ± 198	98

Table S5. Summary of kinetic and catalytic performances of catalysts **2** and **7** for multiple addition tests (water solution at pH 7 by phosphate buffer, 25°C).

Experiment	[Cat] (μM)	[$NaIO_4$]/[$I O_4^-$] (mM)/(mM)	TOF_{max}(X) (min^{-1})	TON	Yield (%)
			$[Cp^*IrCl_2]_2$ (**2**)		
1 (RUN I)	5.0	20.0/0.0	305 ± 31 (0.13)	2023 ± 101	100
1' (RUN II)	5.0	20.0/20.0	204 ± 20 (0.09)	1904 ± 95	93
1'' (RUN III)	5.0	20.0/40.0	150 ± 15 (0.10)	1991 ± 100	99
2 (RUN I)	5.0	20.0/1.0	302 ± 30 (0.16)	1988 ± 99	99
2' (RUN II)	5.0	20.0/21.0	211 ± 21 (0.09)	1983 ± 99	99
3 (RUN I)	5.0	20.0/5.0	250 ± 25 (0.15)	2035 ± 102	102*
3' (RUN II)	5.0	20.0/25.0	201 ± 20 (0.10)	2005 ± 100	100
4 (RUN I)	5.0	20.0/10.0	241 ± 24 (0.10)	1977 ± 99	99
4' (RUN II)	5.0	20.0/30.0	174 ± 17 (0.09)	2009 ± 100	102
5 (RUN I)	5.0	20.0/20.0	196 ± 20 (0.14)	2005 ± 100	100
6 (RUN I)	5.0	20.0/40.0	149 ± 15 (0.09)	1991 ± 100	100
6' (RUN II)	5.0	20.0/60.0	122 ± 12 (0.07)	1987 ± 99	99
			$[\{\eta^5\text{-}C_5Me_4(4\text{-}C_6H_4F\}IrCl_2]_2$ (**7**)		
1 (RUN I)	5.0	20.0/0.0	141 ± 14 (0.08)	2044 ± 105	101*
1' (RUN II)	5.0	20.0/20.0	100 ± 10 (0.07)	2003 ± 100	100
1'' (RUN III)	5.0	20.0/40.0	79 ± 8 (0.09)	2062 ± 103	101*
2 (RUN I)	5.0	20.0/10.0	129 ± 13 (0.11)	2008 ± 100	100
2' (RUN II)	5.0	20.0/30.0	103 ± 10 (0.06)	2005 ± 100	100
3 (RUN I)	5.0	20.0/20.0	97 ± 10 (0.1)	1963 ± 98	98
3' (RUN II)	5.0	20.0/40.0	81 ± 8 (0.6)	1957 ± 98	97

Figure S23. ^{1}H NMR spectrum (400 MHz, $CDCl_3$) of $C_5HMe_4(4\text{-}C_6H_4F)$.

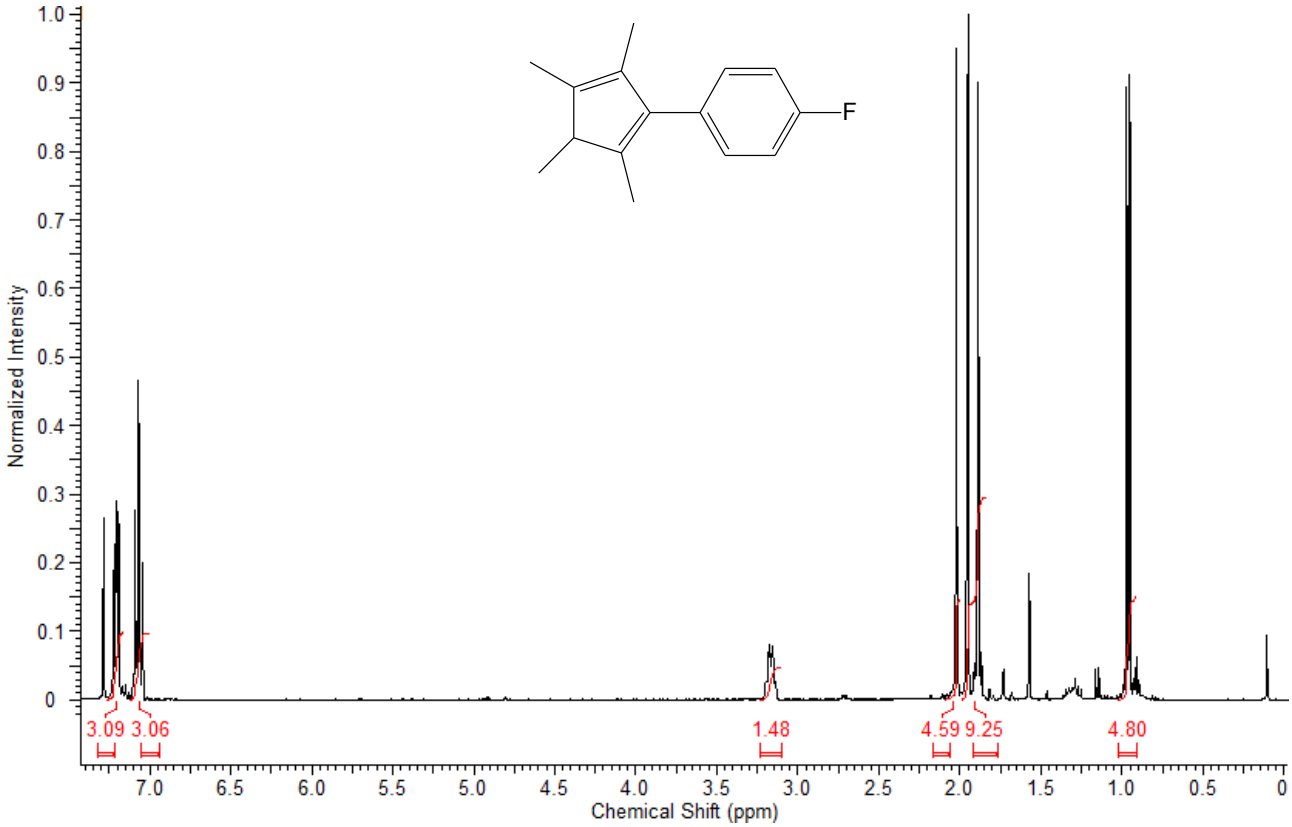

Figure S24. $^{13}C\{^{1}H\}$ NMR spectrum (400 MHz, $CDCl_3$) of $C_5HMe_4(4\text{-}C_6H_4F)$.

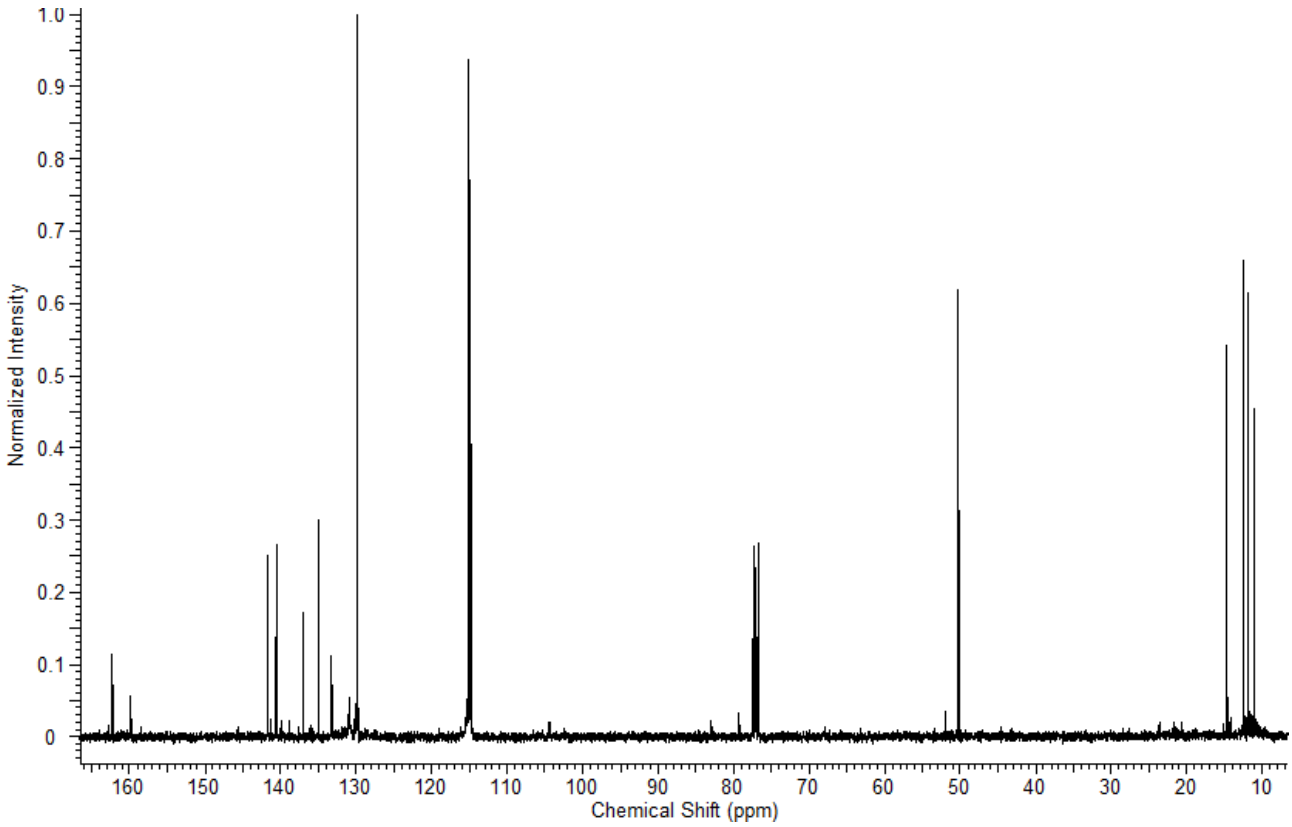

Figure S25. $^{19}F\{^{1}H\}$ NMR spectrum (400 MHz, $CDCl_3$) of $C_5HMe_4(4\text{-}C_6H_4F)$.

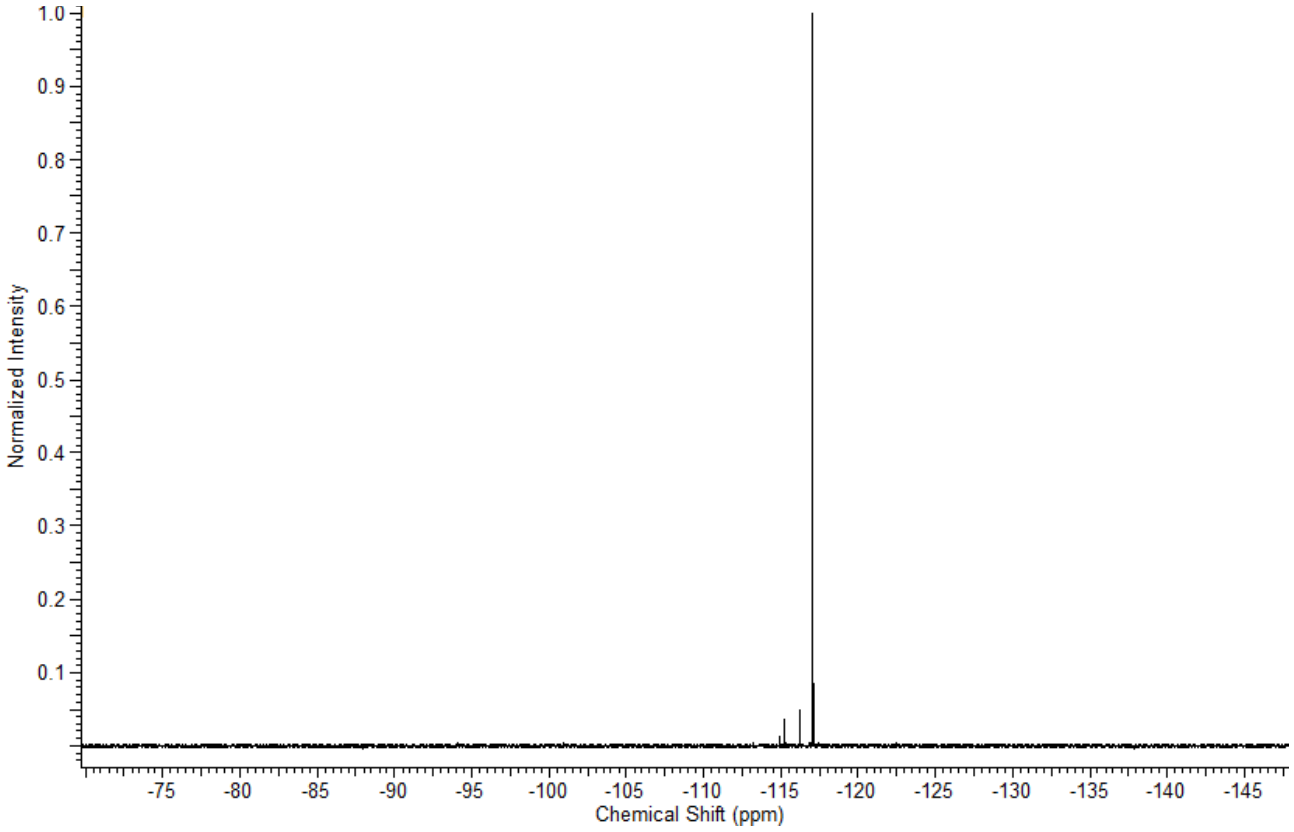

Figure S26. ^{1}H NMR spectrum (400 MHz, $CDCl_3$) of **1**.

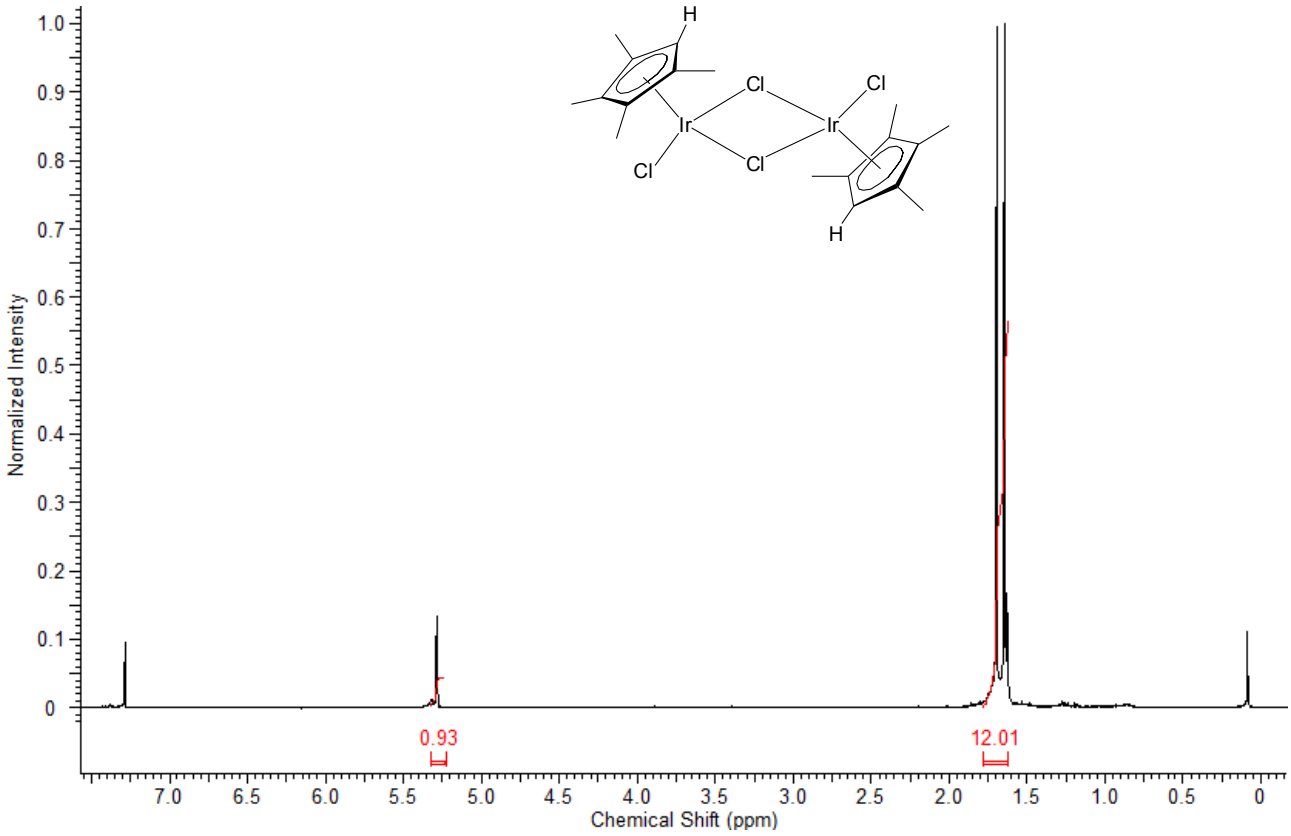

Figure S27. $^{13}C\{^{1}H\}$ NMR spectrum (400 MHz, $CDCl_3$) of **1**.

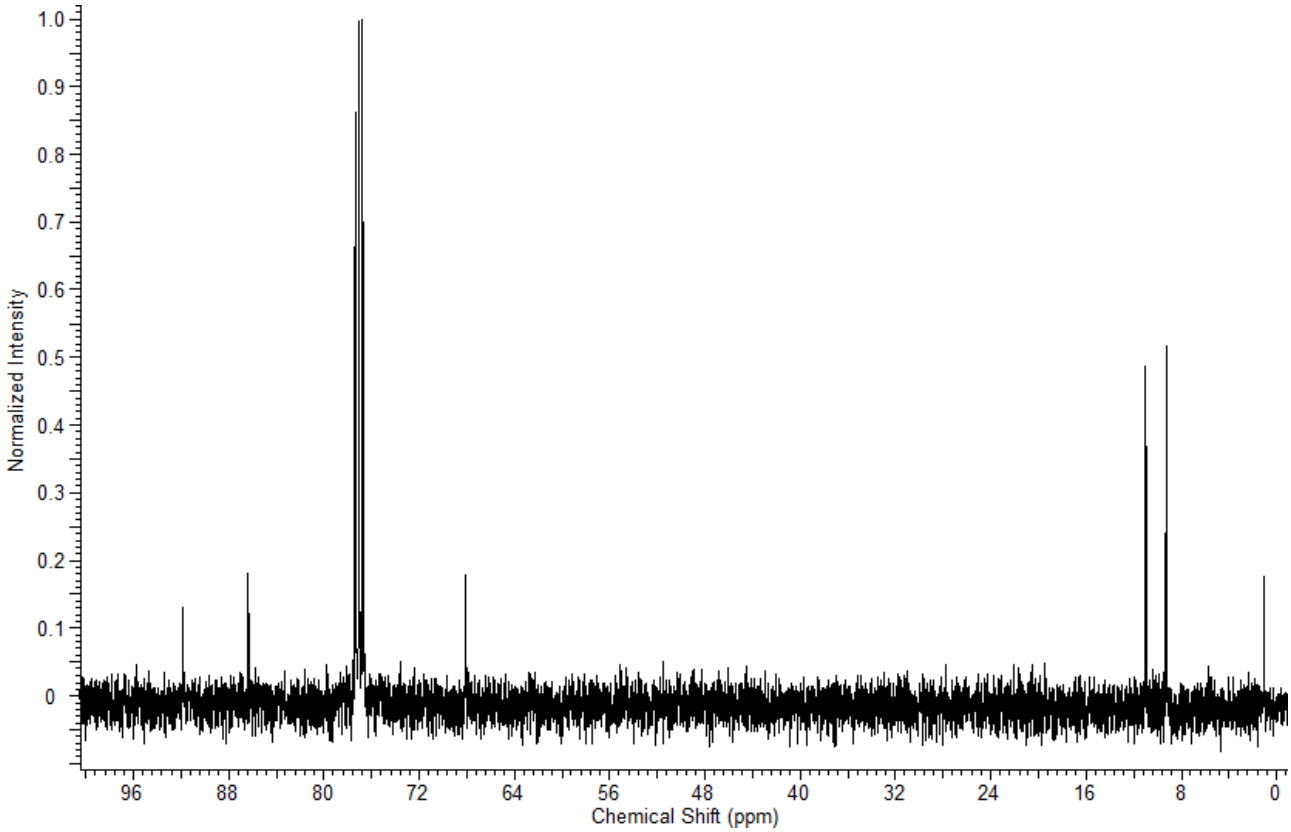

Figure S28. ^{1}H NMR spectrum (400 MHz, $CDCl_3$) of **3**.

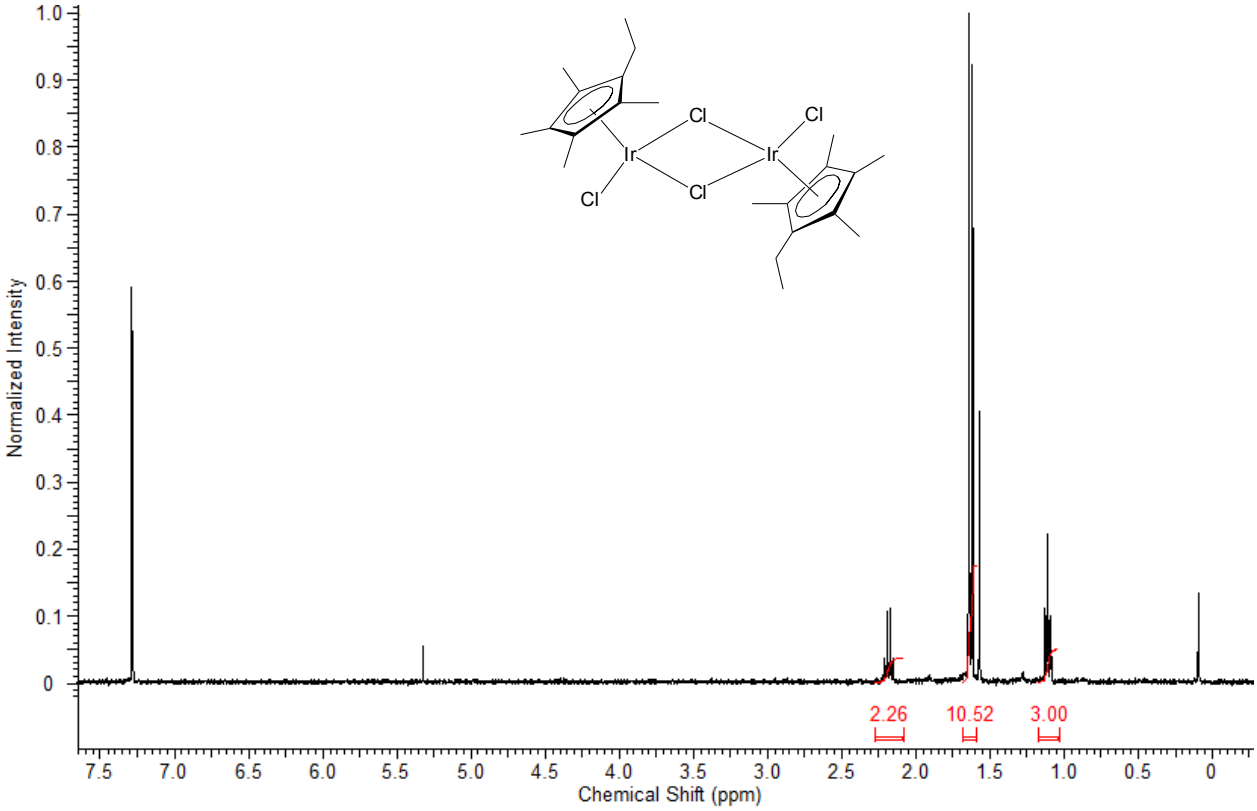

Figure S29. $^{13}C\{^{1}H\}$ NMR spectrum (400 MHz, $CDCl_3$) of **3**.

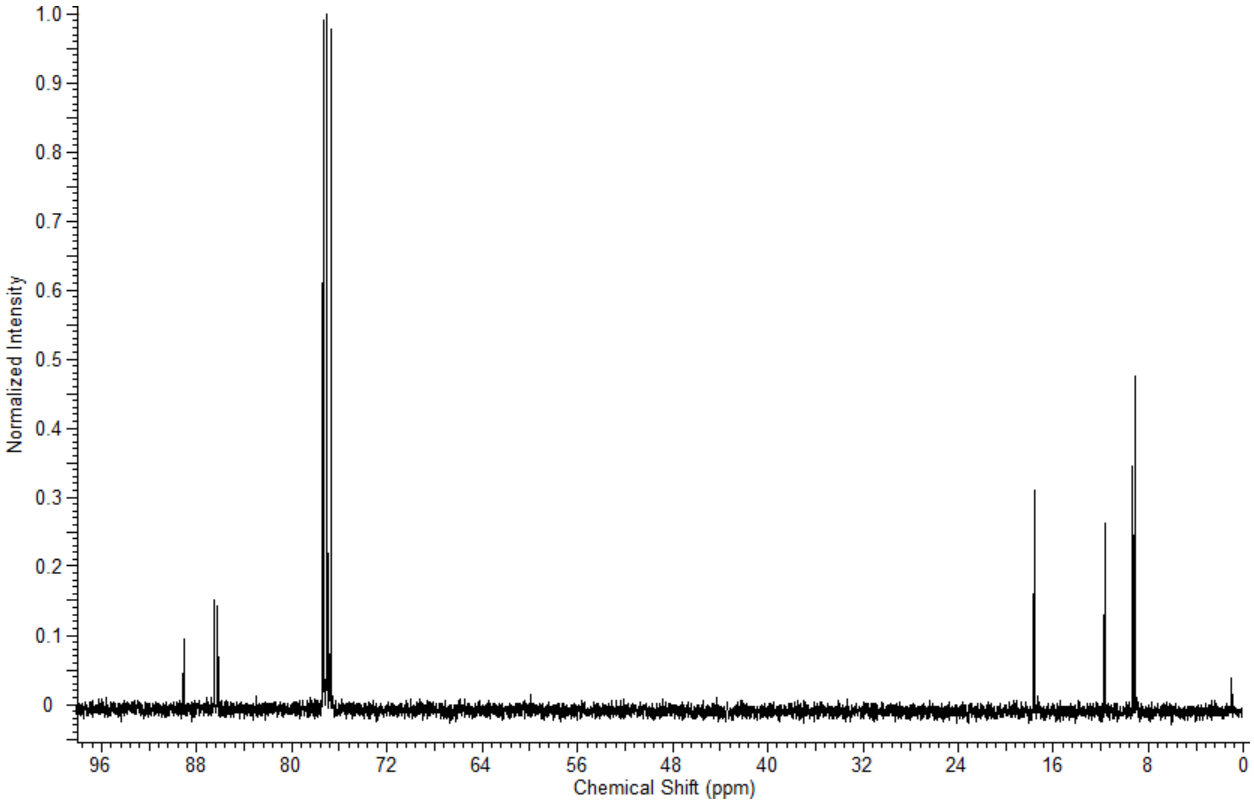

Figure S30. ^{1}H NMR spectrum (400 MHz, $CDCl_3$) of **4**.

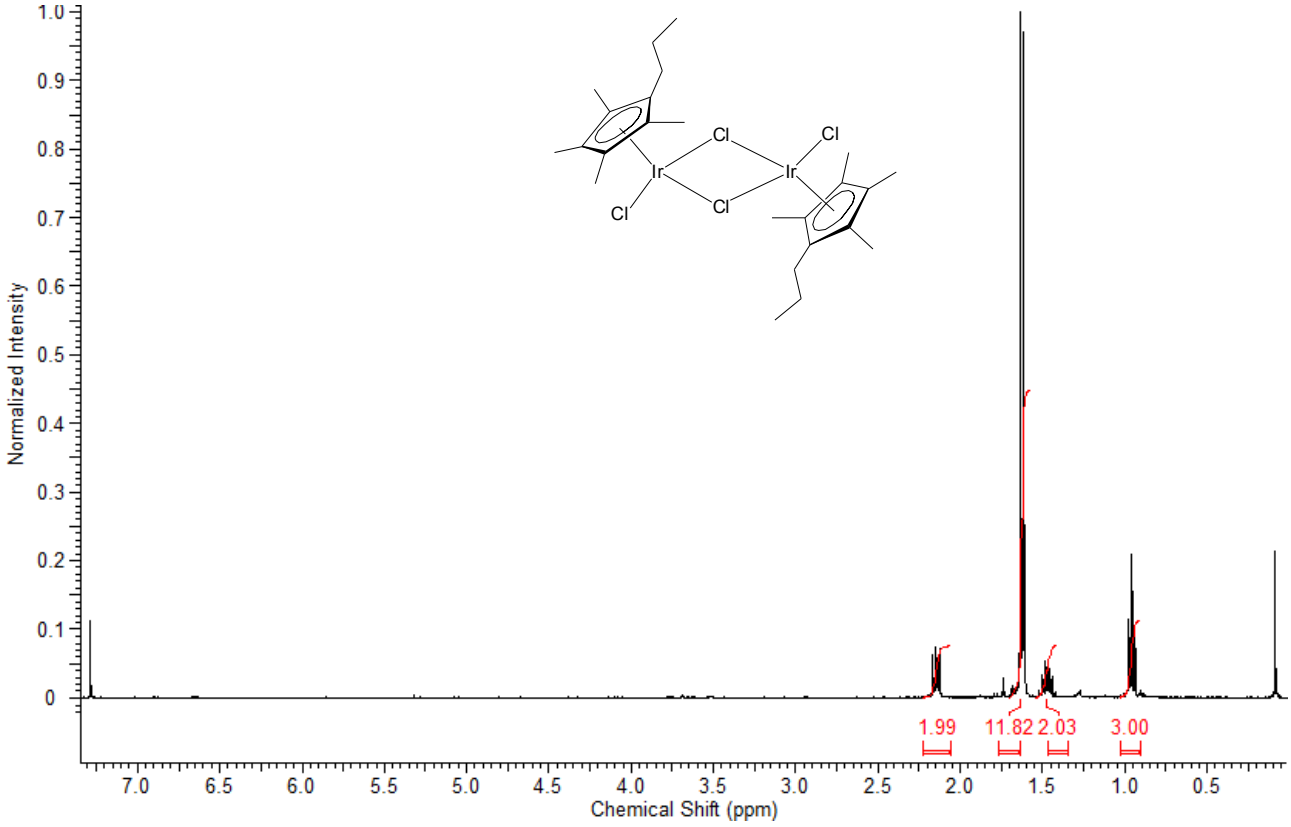

Figure S31. $^{13}C\{^{1}H\}$ NMR spectrum (400 MHz, $CDCl_3$) of **4**.

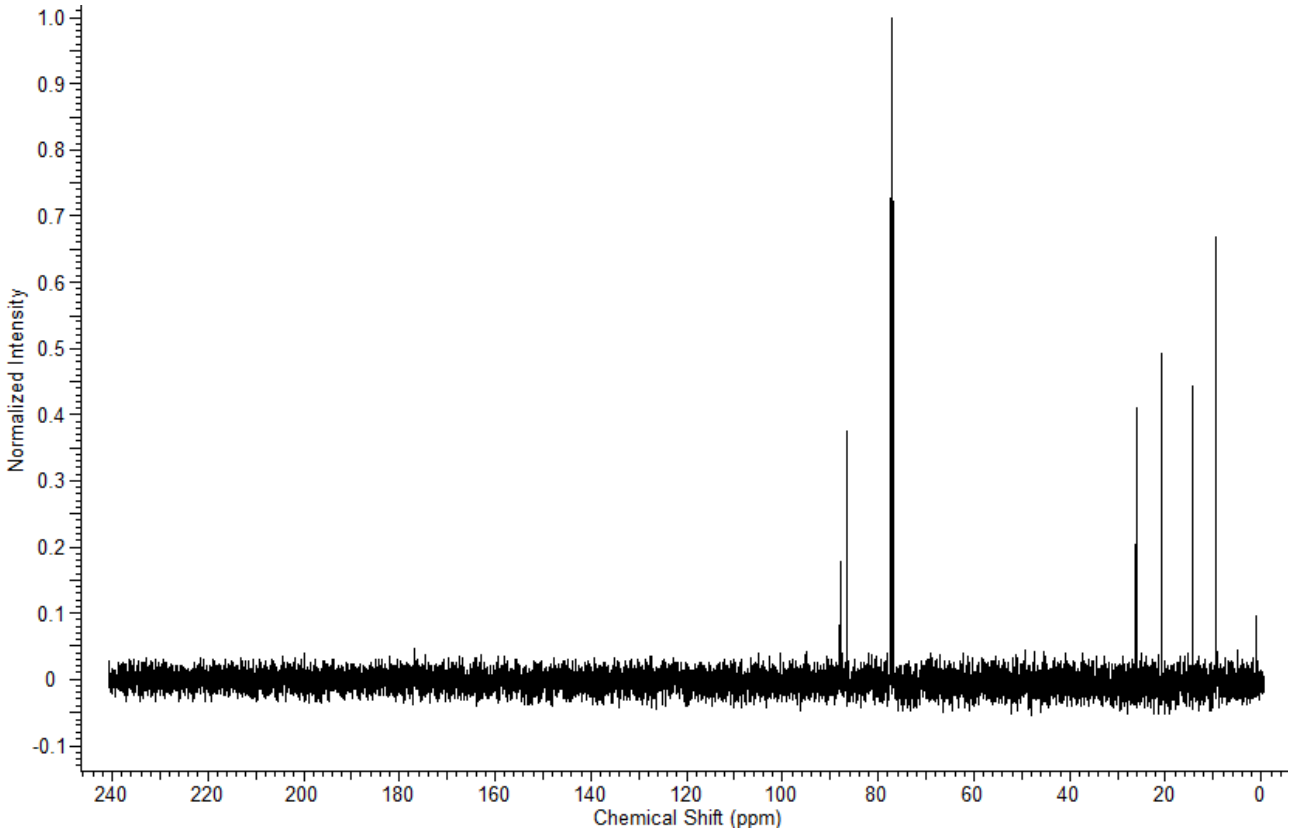

Figure S32. ^{1}H NMR spectrum (400 MHz, $CDCl_3$) of **7**.

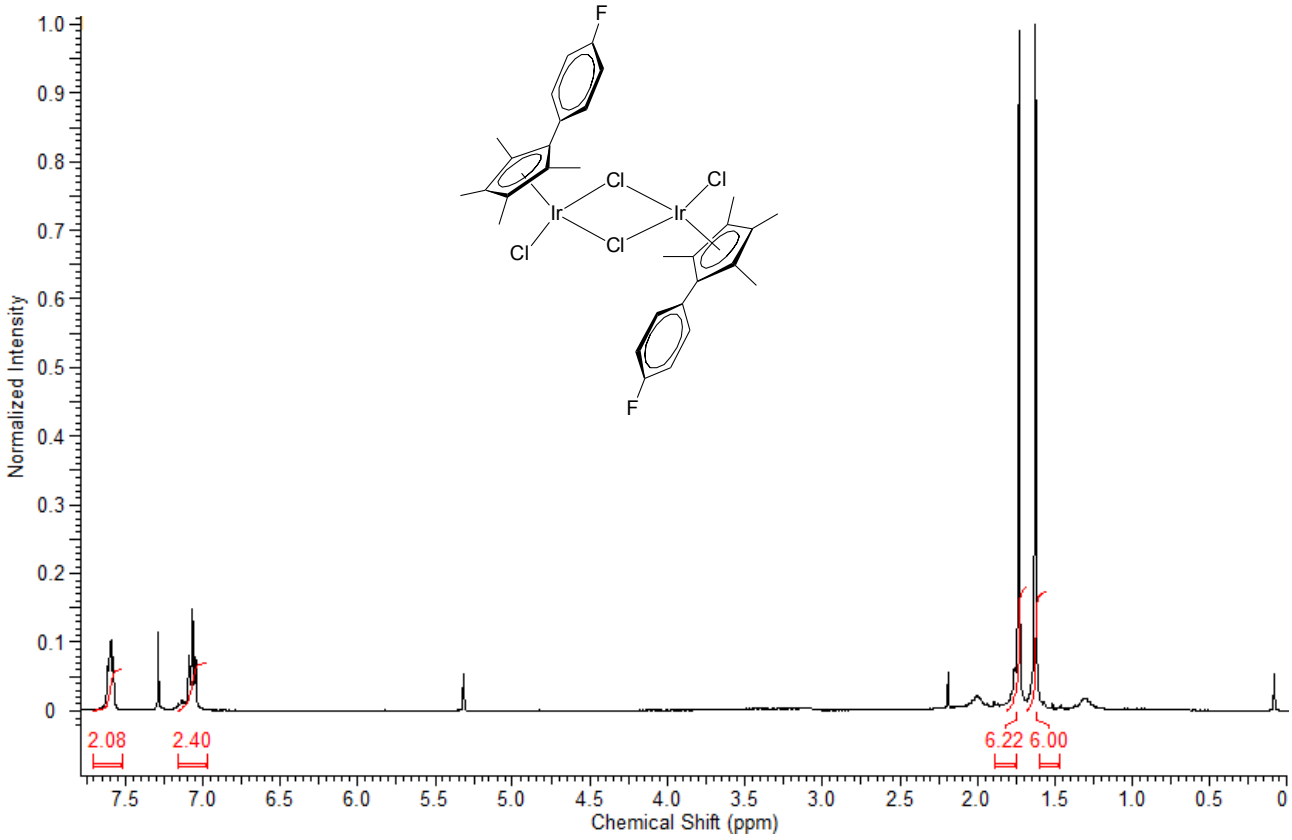

Figure S33. $^{13}C\{^{1}H\}$ NMR spectrum (400 MHz, $CDCl_3$) of **7**.

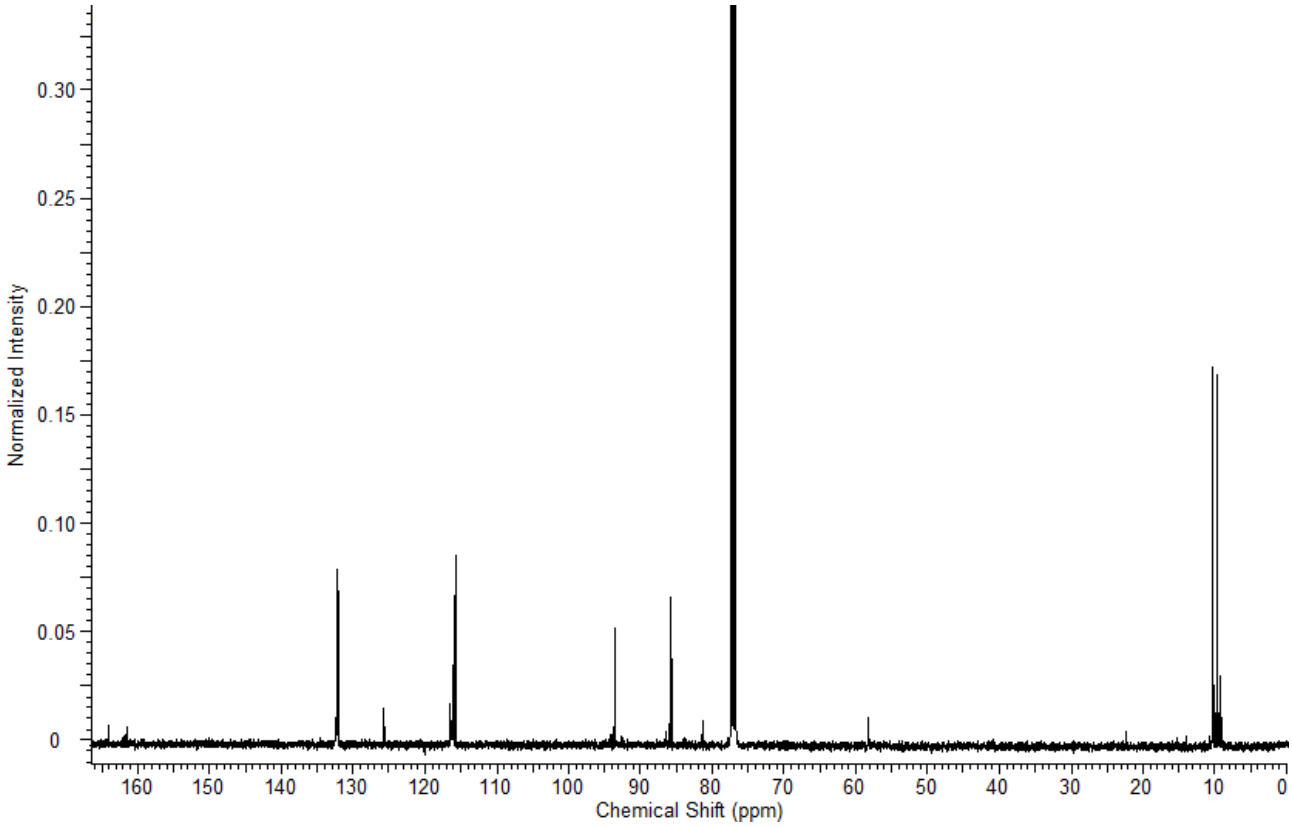

Figure S34. ^{19}F NMR spectrum (400 MHz, $CDCl_3$) of **7**.

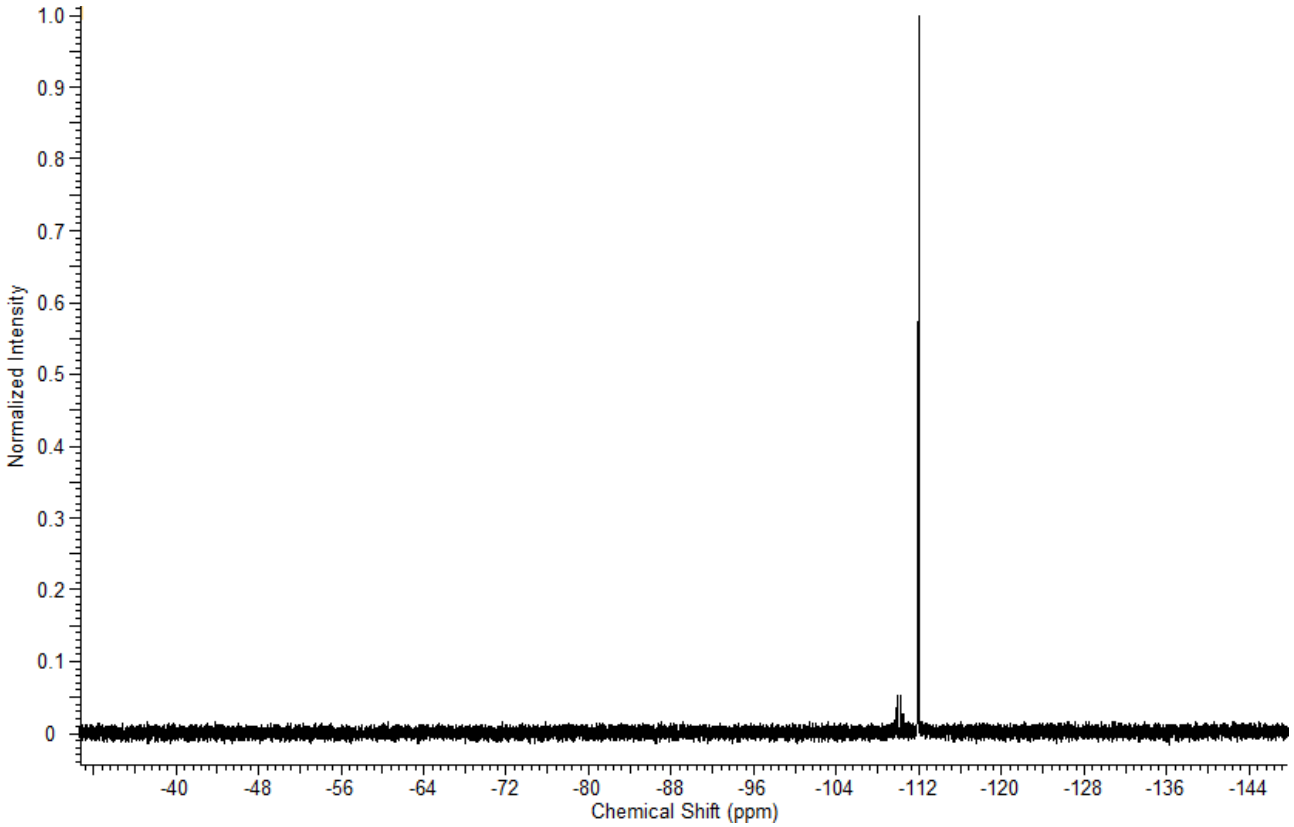

Figure S35. ^{1}H NMR spectrum (400 MHz, CD_3OD) of **8**.

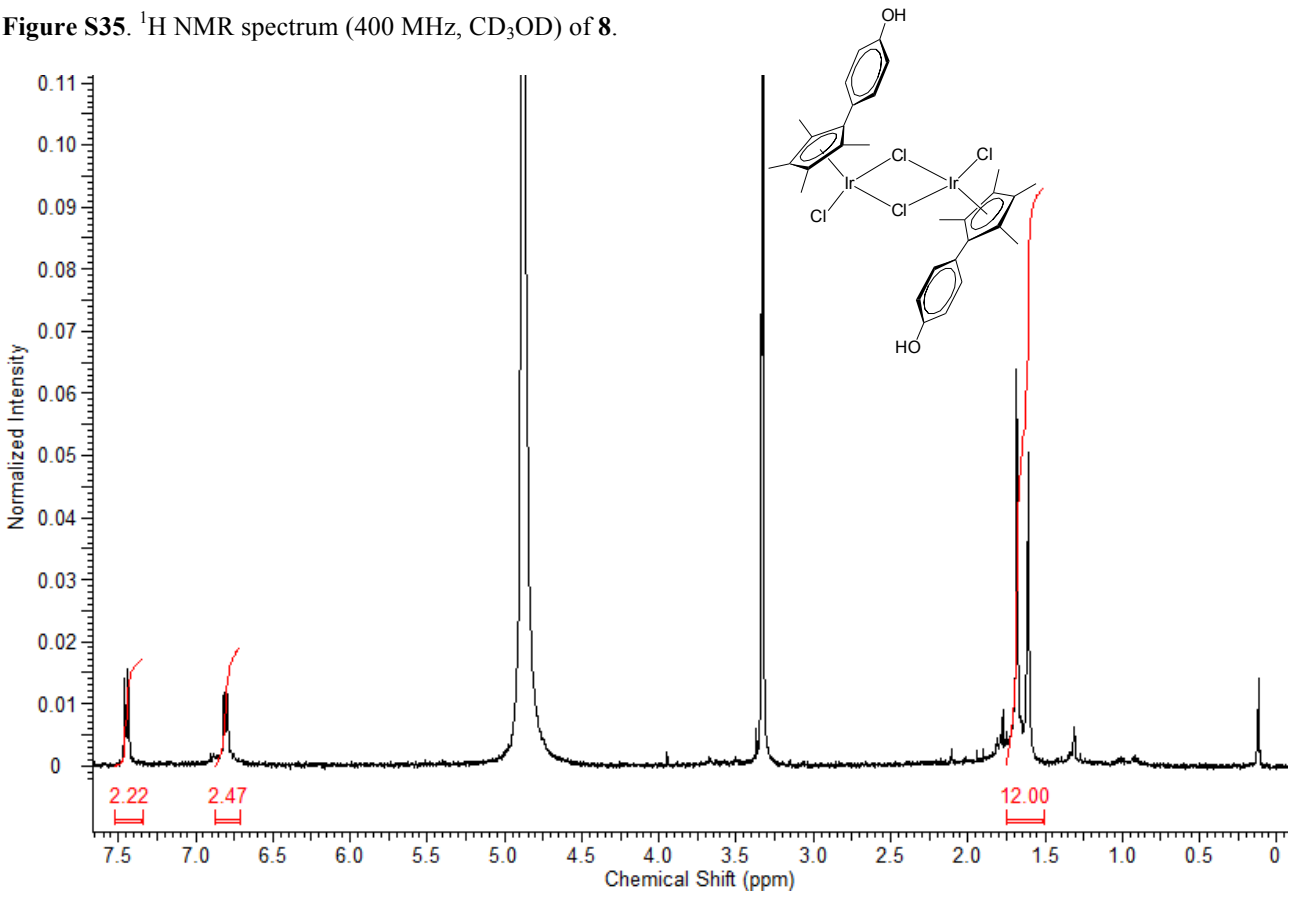

Figure S36. $^{13}C\{^{1}H\}$ NMR spectrum (400 MHz, CD_3OD) of **8**.

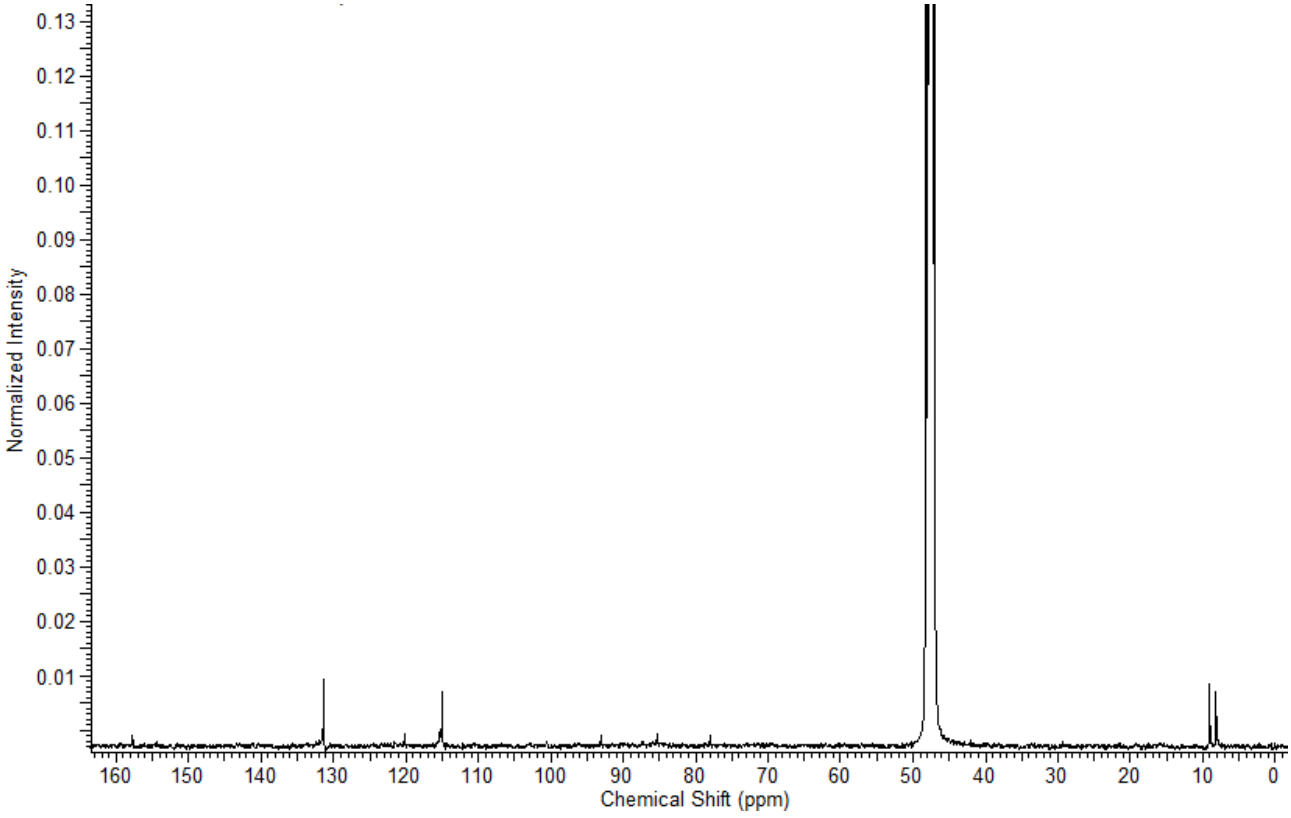

Figure S37. ^{1}H NMR spectrum (400 MHz, dmso-d_6) of **10**.

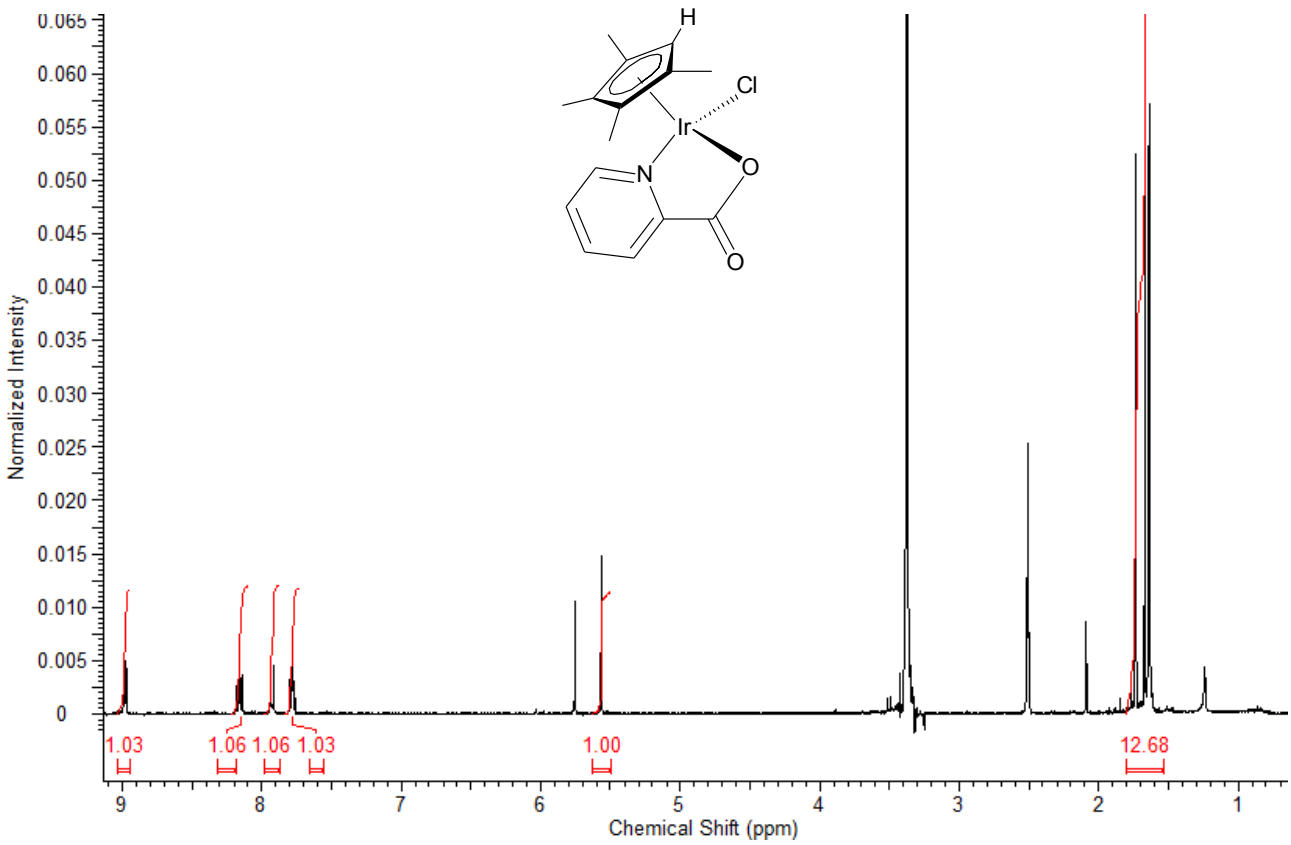

Figure S38. ^{13}C{^{1}H} NMR spectrum (400 MHz, dmso-d_6) of **10**.

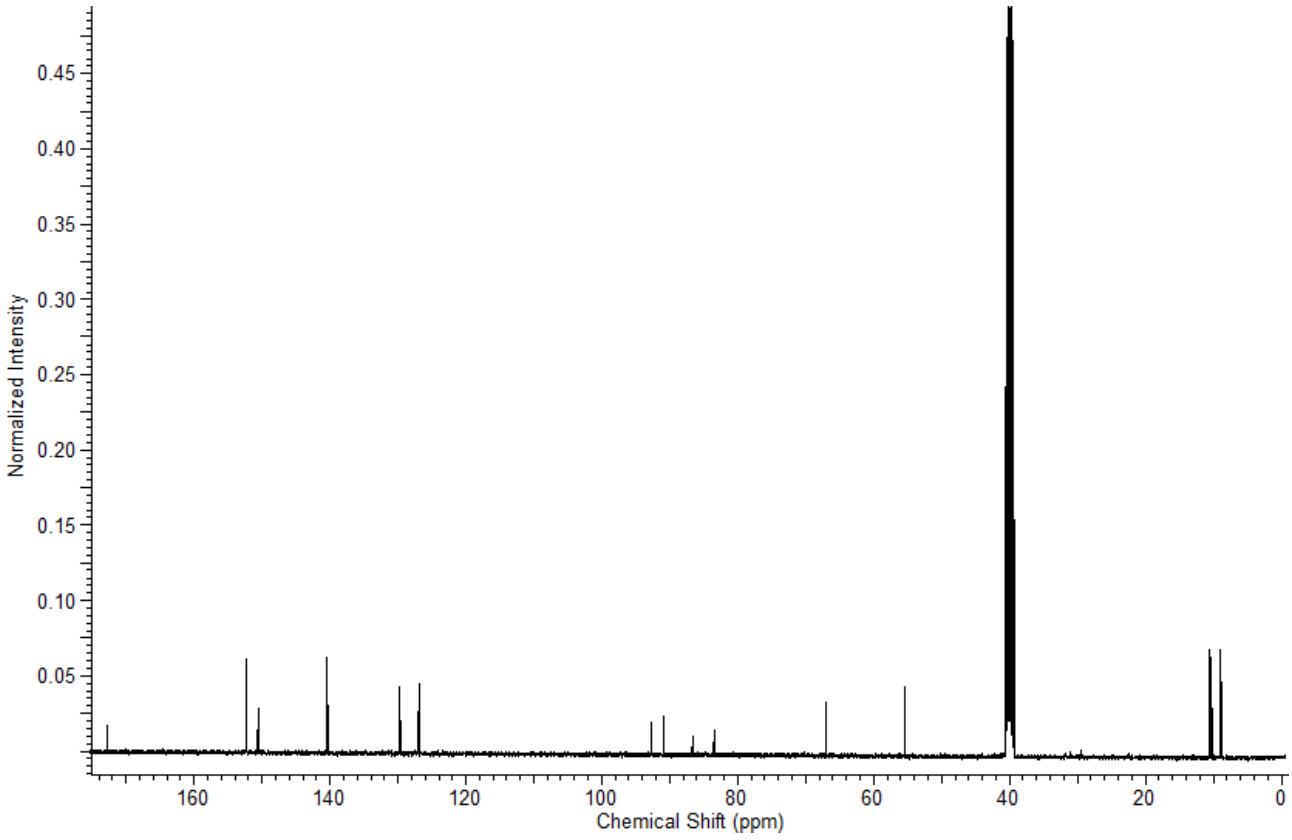

Figure S39. ^{1}H NMR spectrum (400 MHz, $CDCl_3$) of **11**.

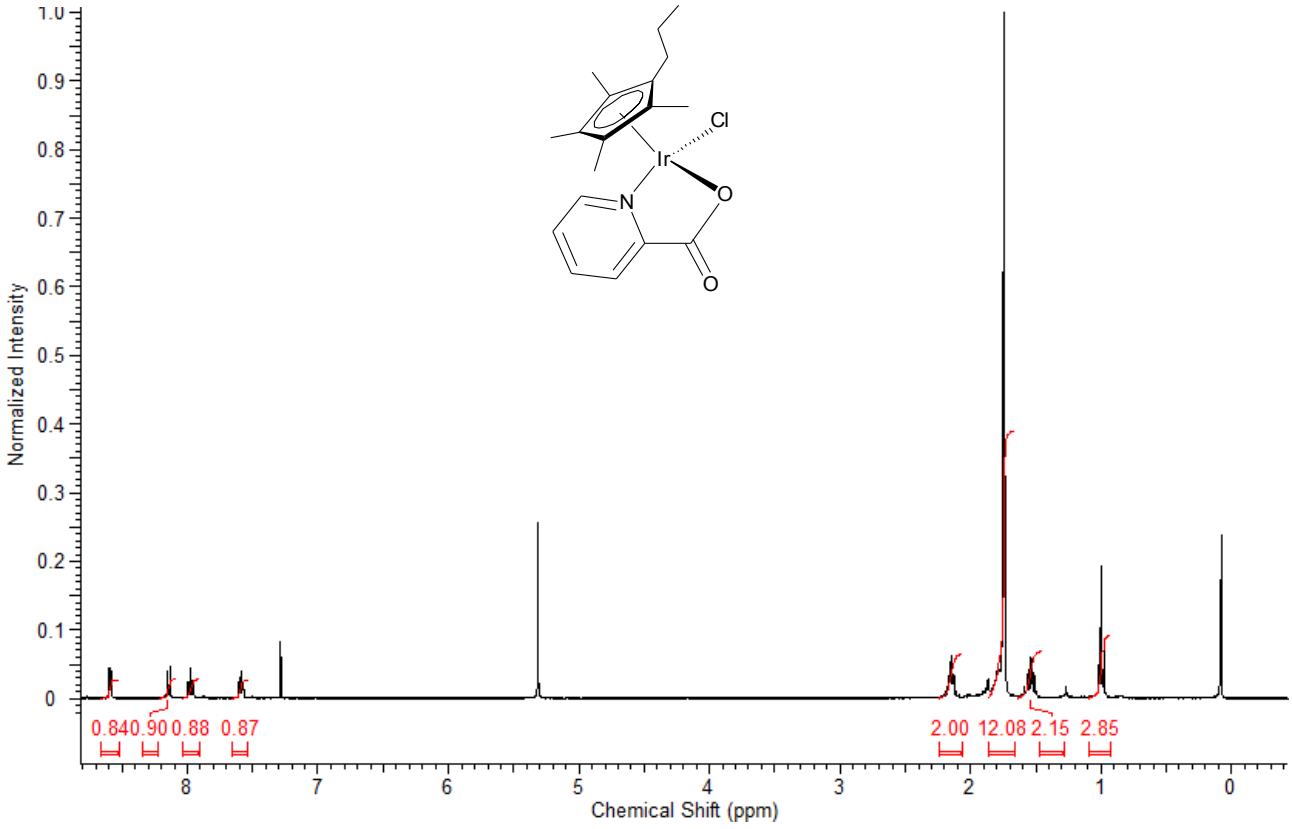

Figure S40. $^{13}C\{^{1}H\}$ NMR spectrum (400 MHz, $CDCl_3$) of **11**.